

Approaches to Solution-Processed Multilayer Organic Light-Emitting Diodes Based on Cross-Linking[†]

Carlos A. Zuniga, Stephen Barlow, and Seth R. Marder*

*School of Chemistry and Biochemistry and Center for Organic Photonics and Electronics,
Georgia Institute of Technology, Atlanta, Georgia 30332-0400, United States*

Received August 20, 2010. Revised Manuscript Received November 16, 2010

The fabrication of multilayer organic light-emitting diodes through solution processing presents challenges, especially regarding dissolution of the first layer during deposition of a second layer. One possible approach to this problem is to insolubilize the first layer using cross-linking. Cross-linking has also been used to control the morphological stability and aggregation phenomena of the active organic materials. In this short review, we discuss the alternative chemically, thermally, and photochemically promoted cross-linking chemistries that have been examined in the context of organic light-emitting diodes including: the hydrolysis of silicon compounds to form siloxanes; the polymerization of styrene, acrylate, and oxetane groups; and the dimerization of trifluorovinyl ethers, benzocyclobutenes, and cinnamates.

Introduction

The study of materials, processing, and devices for organic light-emitting diodes (OLEDs) is a rapidly developing field. OLEDs are of interest partly because of their ability to be processed onto a variety of substrates, their potential for low cost fabrication, and the possibility for fabricating energy-efficient displays and/or solid-state lighting sources.^{1,2} The earliest multilayer OLEDs were reported by Tang and Van Slyke in 1987 and were based on a bilayer architecture.³ Early OLEDs were based on fluorescent organic materials in which emission is only obtained from hole–electron recombination events that result in the formation of singlet excited states, placing limitations on the maximum efficiency of devices.⁴ Use of phosphorescent transition-metal-based emitters, enabling emission from both singlet and triplet excited states, was first reported by Forrest and co-workers in 1999⁵ and has become widespread. Continuing progress in increasing the performance and development of phosphorescent OLEDs has commonly been the result of new complex architectures employing a variety of multilayers with different functions including: hole and electron injection and transport; hole, electron, and exciton blocking; and acting as a host for phosphorescent emitters.^{6,7}

The highest efficiency devices are generally those fabricated using high-vacuum vapor deposition of small-molecule organic materials. This approach permits the fabrication of well-defined multilayers with relative ease. Moreover, small-molecule organic compounds can be highly purified using crystallization and/or sublimation prior to use. Potential drawbacks are the tendency of many small-molecule organic materials to undergo morphological changes, such

as recrystallization, especially at elevated operating temperatures. In some cases, molecules from one layer have been found to diffuse into another during operation.⁸ In addition to these considerations, which can potentially adversely affect device stability and lifetimes, vacuum-processing is also relatively time-consuming and expensive, while fabrication on large-area substrates can also be problematic.² In contrast, solution-based approaches have the potential to facilitate rapid and low-cost processing and can be extended to large-area substrates, and to high-throughput reel-to-reel processing. At the same time, higher molecular-weight materials that cannot be vapor-deposited, such as polymers or oligomers, can show relatively good morphological stability (and presumably resistance to molecular diffusion) relative to small molecules. One drawback with solution processing, at least of higher-molecular-weight materials, is that it is generally more difficult to purify these materials; high material purity is considered to be a critical factor in achieving long-lived devices. Moreover, and of particular relevance to this review, the use of solution-processing to create multilayer architectures can be challenging. In particular, deposition of a second layer from solution can lead to partial dissolution of the preceding layer if the solvent required for the second material also dissolves the first. Careful design and/or selection of materials and solvents so that the solvent for a given layer does not dissolve preceding layers (the so-called “orthogonal solvent” approach) can help circumvent this problem. Indeed, deposition of polymers from organic solvents onto PEDOT-PSS {poly(3,4-ethylenedioxythiophene) poly(styrenesulfonate)}, which is itself typically deposited from aqueous solution and insoluble in organic solvents, is commonly used in device fabrication.^{9,10} Several groups have studied other applications of the “orthogonal solvent” approach but the method is not always practical to implement for a given pair of materials.^{11–15} An alternative approach to

[†] Accepted as part of the “Special Issue on π -Functional Materials”.

*Corresponding author. E-mail: seth.marder@chemistry.gatech.edu.

facilitating multilayer solution processing is to insolubilize an organic material following deposition and prior to deposition of subsequent layers. PPV (poly(*p*-phenylenevinylene)) is an example of an insoluble electroactive material that can be formed from thermal treatment of solution-processed films of a soluble precursor.¹⁶ A more general approach for achieving solubilization subsequent to solution deposition is to incorporate reactive substituents onto soluble electroactive molecules or polymers that, when subjected to thermal, light, or chemical treatments, react to cross-link the film.

This short review will discuss and compare the different functional groups that have been used cross-link active organic materials – both small molecules and polymers – for use in OLEDs. Although several other reviews have discussed aspects of cross-linking for OLEDs,^{17–19} we will discuss additional examples using a wide range of cross-linking chemistries and, in the conclusions, compare the advantages and disadvantages of some of the approaches used to date. For the purposes of this review we will define cross-linking as a process whereby the formation of new covalent bonds leads to insolubilization of an organic layer. Such layers can, therefore, be resistant to degradation by solution-processing of a subsequent layer

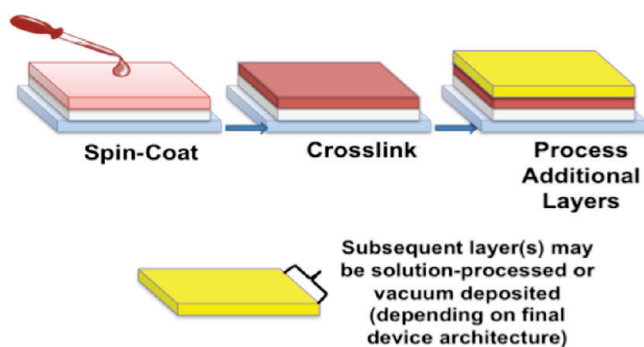


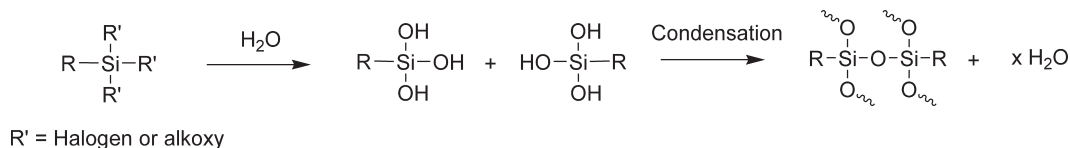
Figure 1. Schematic showing how cross-linking permits solution processing of multilayer OLEDs.

from solution, as shown schematically in Figure 1. The process may be used to fabricate either devices in which the active layers are entirely processed from solution, or “hybrid” OLEDs containing both solution and vacuum-deposited layers. In addition, cross-linking has been used to control other properties of OLED active materials, including morphological stability—for example, to suppress phase segregation or crystallization—and aggregation phenomena.

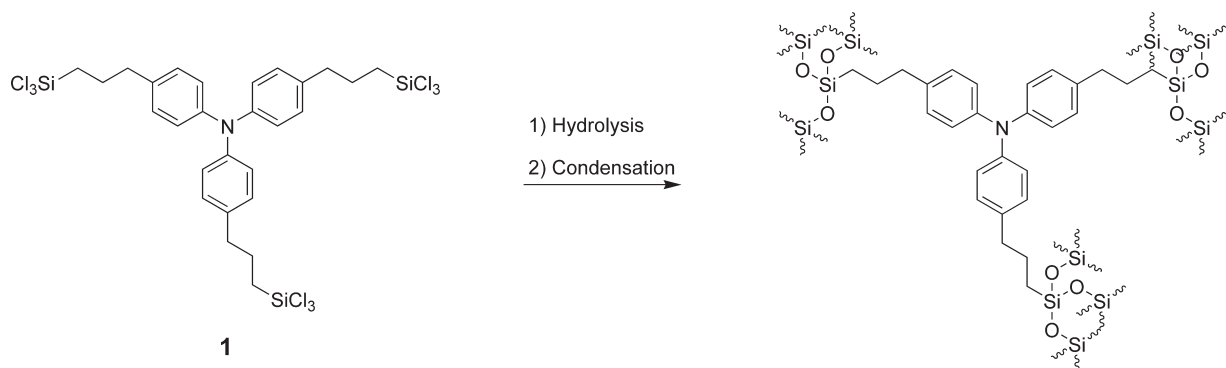
Cross-Linking Chemistries

Siloxanes. The formation of siloxanes from the hydrolysis of halo- or alkoxy-silanes is widely used in materials science. As shown in Scheme 1, the reaction proceeds by hydrolysis, followed by condensation²⁰ of the resulting silanols to give Si–O–Si linkages. Although the process can lead to effective cross-linking and the resulting bonds are very strong and stable, water—either remaining from the hydrolysis step or formed by the condensation – and alcohols or hydrogen halides—from the hydrolysis step—are potential contaminants in cross-linked siloxane films that can potentially impair device performance. The earliest example of the application of siloxane-formation to cross-link an OLED material was reported by Li et al. in 1999.²¹ A tris(trichlorosilyl)-functionalized triarylamine hole-transport material (**1**, Scheme 2) was synthesized that could be easily spin-coated and then cross-linked. The hydrolysis step involved exposure of the layer to moisture followed by a curing step (120 °C) to produce a hard, stable, and adherent film. A “Scotch tape” test was used to confirm resistance to delamination through comparing pre- and post-test UV–vis absorption spectra. Thermogravimetric analysis (TGA) demonstrated very good resistance to thermal decomposition and differential scanning calorimetry (DSC) data showed no thermal events across a range of 50–400 °C, supporting the conclusion of successful cross-linking. Atomic force microscopy (AFM)

Scheme 1. Siloxane-Based Cross-Linking



Scheme 2. Cross-Linking of a Trichlorosilyl-Functionalized Triphenylamine



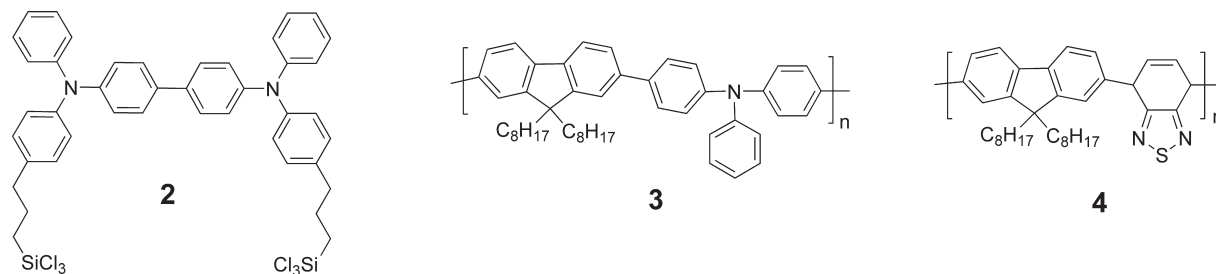


Figure 2. Cross-linkable bis(trichlorosilyl)-functionalized bis(diarylamino)biphenyl derivative and other polymers used along with it in device fabrication.

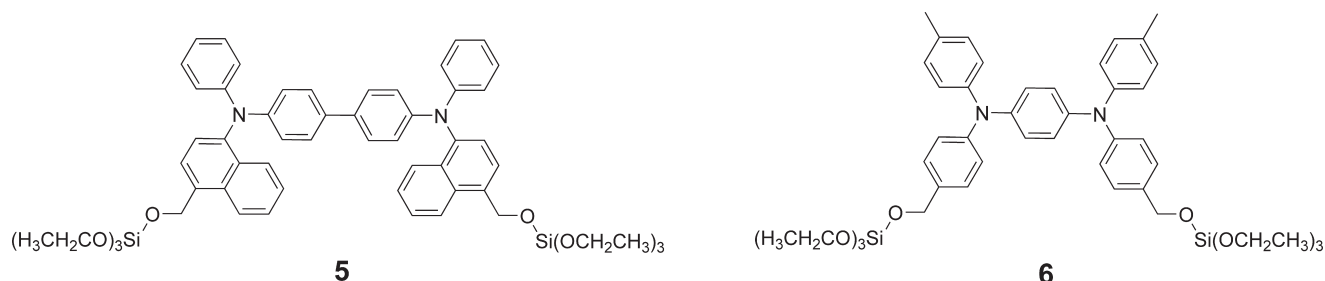


Figure 3. Cross-linkable bis(tri(alkoxy)silyl)-functionalized bis(diarylamino)biphenyl and bis(diarylamino)benzene hole-transport materials.

was used to confirm that the thin films were smooth and defect free. OLEDs were fabricated with the architecture: ITO/cross-linked-**1**/Alq₃/Mg (ITO = indium tin oxide; Alq₃ = tris(8-hydroxyquinolinato)aluminum, vacuum-processed). Device testing showed turn-on voltages of ca. 6 V and average external quantum efficiencies (EQE) of ca. 0.2%. The possibility of trace water or HCl remaining in the hole-transport layer after the curing step was not directly addressed.

Trichlorosilyl groups were utilized by Yan et al.²² to modify bis(diarylamino)biphenyl groups as a cross-linkable electron-blocking material (Figure 2). OLEDs were fabricated in which a blend of **2** and **3** (1:1 by weight) was deposited from toluene onto PEDOT-PSS. These films cross-link spontaneously within seconds of exposure to air to yield a smooth insoluble film. The polymer **4** was then deposited from xylenes as an electron-transport material, resulting in the device architecture: ITO/PEDOT-PSS/**2:3/4**/Ca/Al. Thus, the use of cross-linking enabled fabrication of a device in which all the organic layers were solution-processed. The current density at a given field in the cross-linked device was ca. three times lower than that in a reference device omitting the cross-linkable layer (i.e., ITO/PEDOT-PSS/**4**/Ca/Al), whereas the current efficiency was an order of magnitude higher, demonstrating how cross-linking can facilitate the fabrication of better devices.

Tri(alkoxy)silyl groups have also been used for the cross-linking of hole-transport/electron-blocking materials based on bis(diarylamino)biphenyl and bis(diarylamino)benzene small molecules by Lee et al. (Figure 3).²³ Several cross-linking conditions (using various annealing temperatures) were tested and then evaluated by solvent exposure of the films followed by UV-vis absorption measurements; annealing at 150 °C was found to be necessary to achieve sufficient cross-linking density to insolubilize the layers. AFM studies provided evidence

that the cross-linked films were smooth. Three OLED architectures were employed for the evaluation of the cross-linked layers: I) ITO/PEDOT-PSS/PF/BaF₂/Ca/Al, II) ITO/PEDOT-PSS/**6**/PF/BaF₂/Ca/Al, and III) ITO/PEDOT-PSS/**5**/PF/BaF₂/Ca/Al where PF is a poly(fluorene) derivative that was spin-coated from solution. Electroluminescence (EL) measurements showed only minor changes between the emission color of the devices. Devices II and III had lower current densities than I at a given voltage and showed ca. 30% greater current efficiencies, but the turn-on voltages were higher. Thus, this provides another example of the use of siloxane formation to help in the fabrication of more efficient multilayer devices. However, in none of these siloxane cross-linkable systems has the effect of the cross-linking groups on electronic behavior been investigated by a comparison of cross-linked and non-cross-linked materials and so the potential impacts of side-products of the cross-linking reaction are unclear.

Styrenes. Styrenes are well-known to undergo polymerization through both radical and anionic mechanisms. In particular, the radical polymerization can be thermally initiated. Thus polymerization of styrenes can potentially serve as a method for thermally cross-linking OLED materials. A small molecule functionalized with a single styrene moiety will yield a linear polymer (which may well be soluble) and so candidates for cross-linking are typically functionalized with at least two styrene groups. The method has also been applied to polymers, both by incorporating the styrene groups as end groups or as side groups (Scheme 3). Attractive features of styrene chemistry, in contrast to the siloxane chemistry discussed above, is that no additional reagents are required and no side products are anticipated, besides those associated with chain terminations. However, the functional organic materials must be stable at the temperatures required for cross-linking and relatively unreactive toward the propagating polymer chain.

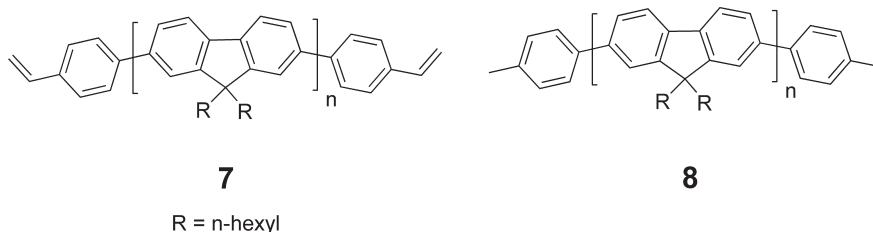
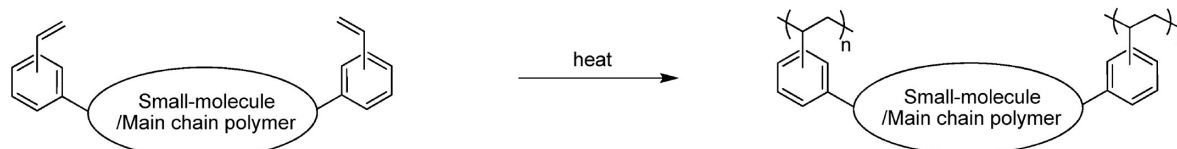


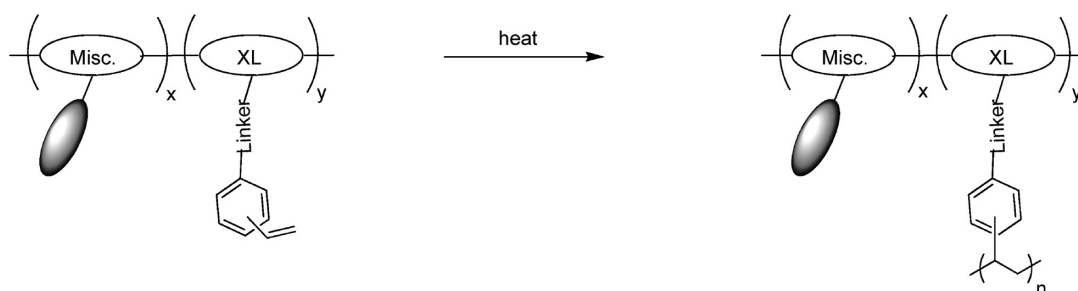
Figure 4. Cross-linkable polyfluorene and an analogous non-cross-linkable homopolymer.

Scheme 3. Thermally Initiated Cross-Linking of Styrene-Functionalized Molecules and Polymers

End-Group Functionalization:



Side-Group Polymer Functionalization:



A considerable body of work with styrene cross-linking groups has been concerned with using cross-linking as a means of controlling the emission properties of polyfluorenes. Pure polyfluorenes are blue emitters in solution, but additional red-shifted emissions shown in the solid state have generally been attributed to the formation of intrachain aggregates, exciplexes, and/or excimers²⁴ (with fluorenone impurities also playing a role in some cases²⁵). In 1999, Miller and co-workers²⁶ synthesized cross-linkable oligo- and poly(dialkylfluorenes) of varied molecular weights (**7**, Figure 4) by Ni⁰-coupling of the appropriate dibromofluorenes and end-capping with 4-bromostyrene. Non-cross-linkable analogues (**8**) were obtained by end-capping the polymerization with 4-bromotoluene. TGA showed no significant weight loss up to ca. 400 °C. Cross-linking was monitored through using in situ IR spectroscopy, DSC, and thin-film solubility tests. The disappearance of the vinyl group C=C and vinyl C-H modes with increased thermal annealing time and the insolubility of the resulting thin-films in chloroform (as evidenced by their UV-vis spectra) were suggestive of cross-linking. DSC of an uncross-linked polymer ($M_n = 3500$) showed a glass-transition, T_g , of 80 °C on the first heating and an exothermic transition at ca. 175 °C. Subsequent heating cycles showed increasingly high T_g values, as well as the disappearance of the exothermic peak, which also supported the conclusion that a thermal cross-linking event had occurred. To establish the effects of cross-linking on excimer/exciple and/or aggregation effects, thin films of **7** and **8** were prepared and annealed at 200 °C for 12 h.

Their photoluminescence (PL) spectra revealed little change in the emission on annealing of **7**, while the non-cross-linkable **8** shows a marked red shift in emission after annealing; the red-shifted peak was attributed to aggregate formation on annealing, with the cross-linking of **7** inhibiting this aggregation. Single-layer OLEDs (ITO/**7** or **8**/Ca) were fabricated. The EL spectra for **8** showed a red-shifted emission peak similar to that seen in the PL data. Although the excimer emission peak was less significant in comparison to the PL data, this could be attributed to the use of a higher molecular-weight sample of **8**. The authors suggested that the degree of excimer/exciple/aggregate formation is dependent on the polymer's molecular weight, with higher-molecular-weight samples exhibiting lower chain mobility, resulting in suppression of intermolecular ordering and limited excimer formation. For **7**, the relatively weak bathochromically shifted EL peak was explained in terms of the effect of cross-linking in preventing the polymer ordering upon annealing. The authors noted that decreased reactivity of the cross-linking styrene end groups with increasing molecular weight and that for $M_n > 30$ kDa cross-linking suppressed excimer formation less effectively. A polymer weight range of 3–5 kDa was suggested to be ideal for cross-linking of these polymers. However, polymers at the low-molecular-weight end of this range may not form high-quality thin films. In the same study, vinyl benzyl cross-linking moieties were also incorporated into the side-chains of a poly(dialkylfluorene) main-chain polymer, **9** (Figure 5). Depending on the molecular

weight, this second class of cross-linkable polymer was also found to become insoluble upon annealing at 200 °C for 10–60 min. PL data showed that cross-linking of this type of compound was unable to suppress bathochromically shifted emission peaks.

In 2001, Carter and co-workers²⁷ reported cross-linkable amorphous poly-2,7-fluorene networks as a means of limiting aggregation and excimer/excimer effects, as well as permitting the processing of multilayers. In order to fabricate blue OLEDs, copolymers of 2,7-fluorene and a spiro-bifluorene compound were prepared with various molecular weights and end-capped with styryl groups (**10**, Figure 6). The spiro-bifluorene was introduced to impart amorphous properties with high T_g values; indeed, increasing values of T_g were observed for polymers with increased spiro-bifluorene content. Thin films of polymer **10** ($M_n = 3.8$ kDa) were prepared and thermally cross-linked at 120 °C for 30 min. Thin-film PL data for this polymer in both its cross-linked and uncross-linked states show suppression of aggregate emission, while that of the corresponding non-cross-linkable homopolymer, poly-2,7-(9,9-dihexylfluorene) showed a red-shifted emission. An OLED (ITO/PEDOT-PSS/**11**/**10**/Ca/Al) {**11** is shown in Figure 7} was fabricated using a higher molecular weight sample of **10** ($M_n = 12.8$ kDa), because of its formation of higher quality films, as the emissive layer and cross-linking this material at 100 °C. The EL spectrum showed no sign of aggregate/excimer emission. The external quantum efficiency (EQE) of the device was reported at 0.08% at 9 V. Based on the low EQE, a device possessing an additional solution-processed electron-transport layer was fabricated. Although this device showed a worse EQE of 0.06%, it illustrated the potential of styrene-

based cross-linking to facilitate the fabrication of multilayer devices.

In 2003 Bozano et al.²⁸ reported an investigation of a blend of two styrene-functionalized cross-linkable polymers. Cross-linking was employed as a possible means of inhibiting the tendency of polymer blends to suffer from phase-segregation effects.²⁹ The blend of a blue-emitting polyfluorene with styryl end-capping groups (**7**, Figure 4), and a polymeric triarylamine hole-transport material with the same styrene end groups, **11** (Figure 7) was compared to a blend of non-cross-linkable analogues terminated with 4-butylphenyl groups. Thin films on silicon wafers were characterized by AFM and both cross-linkable and non-cross-linkable polymer blends were cured at 150 °C under nitrogen. AFM data (Figure 8) indicated that a non-cross-linkable single layer blend of **7** and **11** analogues suffered significant phase segregation, whereas this was considerably diminished in the cross-linked blend. Films (single component or cross-linkable blends) were also fabricated on top of a cross-linked **11** layer. For both these double-layer samples, relatively smooth films were observed; this observation in the non-cross-linked blend was attributed to adoption of a stratified morphology resulting from the effect of the underlying layer on the top layer. Nevertheless, even for cross-linked blends, some degree of segregation was observed. OLEDs with an architecture: ITO/PEDOT-PSS/active layer(s)/Ca or LiF were fabricated. All devices were thermally annealed (150 °C for 45 min) regardless of whether the polymer in question was cross-linkable or not. For evaluation of single-layer polymer blends, devices containing a blend of cross-linkable **7** and **11** in different ratios were fabricated and compared with a device incorporating a blend

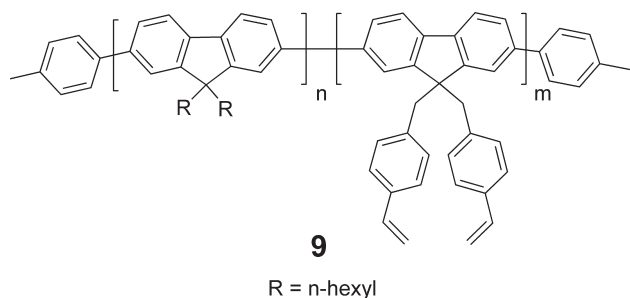


Figure 5. Polyfluorene with cross-linkable vinyl benzyl side groups.

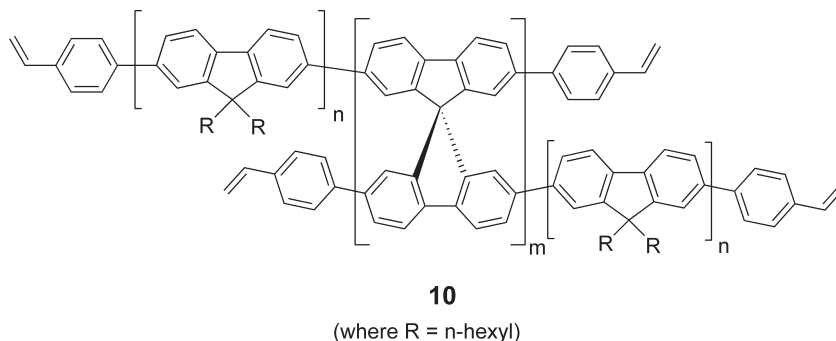


Figure 6. Spiro-linked polyfluorene material with styrene cross-linking groups.

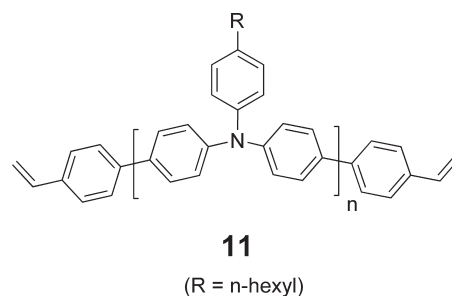


Figure 7. Polymeric triarylamine with terminal styrene cross-linking groups.

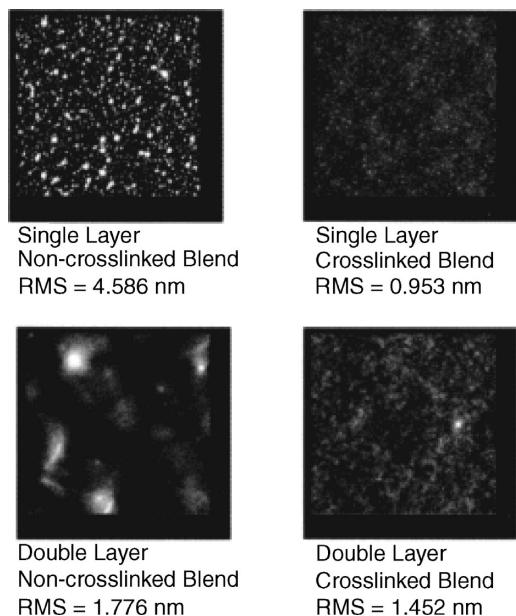


Figure 8. AFM topography images of blends of either cross-linked (“x”) or analogous non-cross-linkable (“n”) layers. Above left: single layer n-7/n-11 (90:10). Above right: single-layer x-7/x-11 (90:10). Below left: double-layer n-7/n-11 (90:10) on top of x-11. Below right: double-layer x-7/x-11 (90:10) on top of x-11. Reproduced with permission from ref 28. Copyright 2003 American Institute of Physics.

of the two analogous non-cross-linkable polymers. Although the cross-linked devices generally exhibited higher leakage currents, they seemed to have a better recombination efficiency, which led to higher radiance than the equivalent devices based on non-cross-linkable blends. Many devices with varying types of blends of both cross-linkable and non-cross-linkable polymers were studied and the EQE data are summarized in Figure 9. Bilayer devices, in which a second layer (single component or blend) was deposited on a layer of cross-linked **11**, showed that the bilayer architecture was in all cases more efficient than the single-layer devices. Overall, the work discussed in this paper showed that cross-linkable blends of polymers could be used as active layers in OLEDs and that, by varying the blend ratios, the device properties and efficiencies could be controlled, thus showing that the blending approach can be a viable alternative to copolymer approaches.

A PPV derivative functionalized with styryl end groups (Figure 10) was studied by Wang and co-workers.³⁰ Although films of PPV itself had previously been made obtained as insoluble films,³¹ the PPV precursor route had the disadvantage of potentially leaving byproducts that could deleteriously affect device performance. By using cross-linkable styryl end-capped PPV polymers bearing solubilizing alkoxy groups, the authors were able to achieve cross-linking while avoiding the potential for forming these side products. Thin-films of the polymer were prepared and thermally cross-linked (175 °C for 1 h); UV-vis spectra before and after solvent washing indicate that cross-linking results in an insoluble film, whereas AFM showed the cross-linked films to have a generally smooth texture. Device properties of the cross-linkable

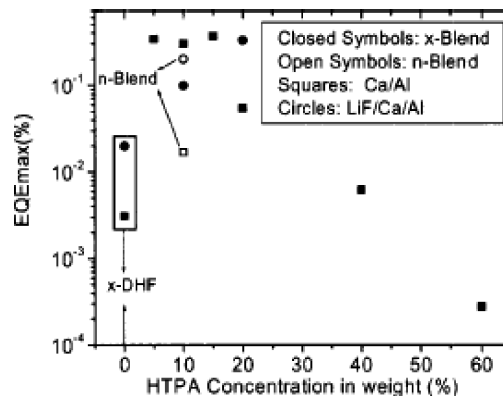


Figure 9. EQE measurements of OLEDs based on cross-linked blends of **6** and **11** (x-blends) and blends of their non-cross-linkable analogues (n-blends); DHF and HTPA denote **6** and **11** (and their non-cross-linkable analogues) respectively. Reproduced with permission from ref 28. Copyright 2003 American Institute of Physics.

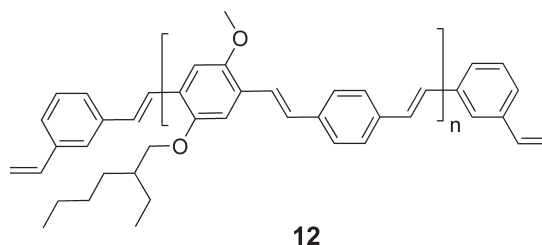
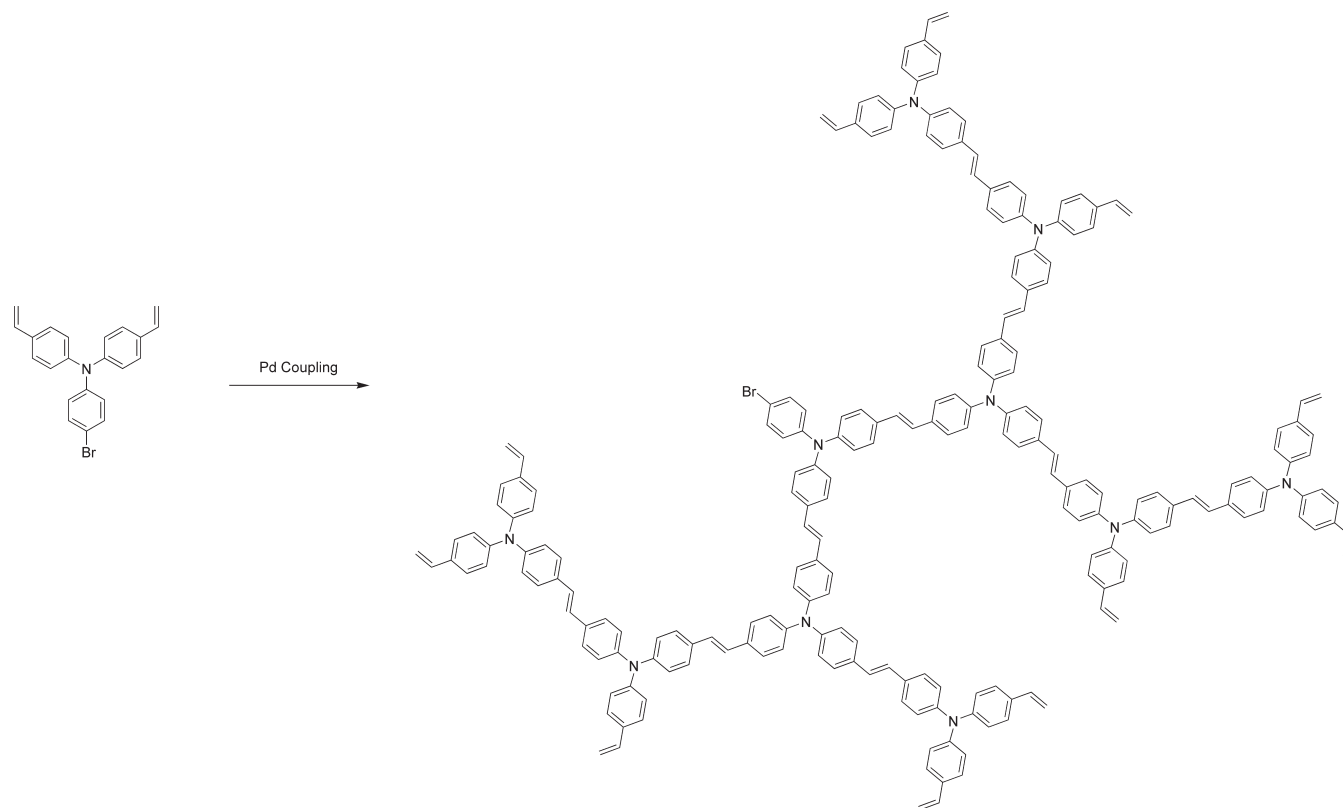


Figure 10. PPV derivative with cross-linkable styrene termini.

PPV derivatives were evaluated in two OLEDs devices. The first was a single-layer device possessing the architecture: ITO/PEDOT-PSS/cross-linked-**12**/Ca/Al. The device emitted in the yellow-green with a low luminance efficiency of 0.054 cd/A. The second device was a double-layer device made possible by the cross-linking of the PPV layer and incorporated an electron-transport layer composed of a polymethacrylate with oxadiazole side chains between the cross-linked PPV and Ca/Al layers. This second device had a reported luminance efficiency of 0.7 cd/A, which is a marked improvement over that of the single layer device.

In 2006, Paul et al.³² reported on a cross-linkable hyperbranched triarylamine-based hole-transport material (**13**, Scheme 4). The material was synthesized by Heck coupling as shown in Scheme 4. TGA data showed that the non-cross-linked polymer was stable up to 350 °C under argon. DSC showed a single exothermic transition at 150 °C on the first scan that disappeared in subsequent scans and was taken as evidence of polymerization. On the basis of the DSC results, thin films were cross-linked at temperatures above 150 °C to form a three-dimensional polymer network. UV-vis spectroscopy was used to compare the resistance of cross-linked films to washing with tetrahydrofuran to that of the non-cross-linked material. A bilayer OLED was fabricated with the architecture: ITO/cross-linked-**13**/MEH-PPV/Ca/Al {MEH-PPV = poly-[2-methoxy-5-(2'-ethylhexyloxy)phenylene vinylene]}. This device was compared to an analogous device in which PEDOT:PSS was used in place of the cross-linked hyperbranched material. Both devices were exhibited quite similar EQEs, indicating that

Scheme 4. Representative example of the Type of Hyperbranched Hole-Transport Material Formed by 4-Bromo-4',4''-divinyltriphenylamine under Heck Conditions

13

the cross-linked material was able to function as an adequate hole-transport/injection layer.

In 2007, Jen and co-workers described a di(styrene)-functionalized tris(carbazolyl) triphenylamine derivative, **14**, with the structure and cross-linking chemistry as shown in Scheme 5, as a hole-transporting layer that could be placed between PEDOT-PSS and the solution-processed emissive layer of an OLED³³ (PEDOT-PSS has been reported to partially quench emission from an immediate adjacent emissive layer and the use of inter-layers has previously been reported to improve device performance³⁴). DSC, UV-vis, and AFM (see Figure 11) indicated that cross-linking could be achieved by isothermally heating thin films at 180 or 160 °C for 30 min (the latter failing to cross-link fully). White-emitting phosphorescent OLEDs were fabricated with an overall device architecture as follows: ITO/PEDOT:PSS(60 nm)/cross-linked-**14**(15–34 nm)/EML (30 nm)/TPBI(25 nm)/CsF/Al {EML = blend of blue-, green-, and red-emitting transition-metal phosphors with PVK; TPBI = 1,3,5-tris(*N*-phenylbenzimidazol-2-yl)benzene} were fabricated. The devices were found to possess stable emission with good CIE coordinates in the near-white range; Table 1 summarizes their performance. Devices with **14** showed much better performance than the control with no inter-layer between PEDOT-PSS and the emissive layer, the efficiency increasing and then decreasing at the thickness of the hole-transport layer is increased. The improved performance of the **14** devices was attributed to enhanced

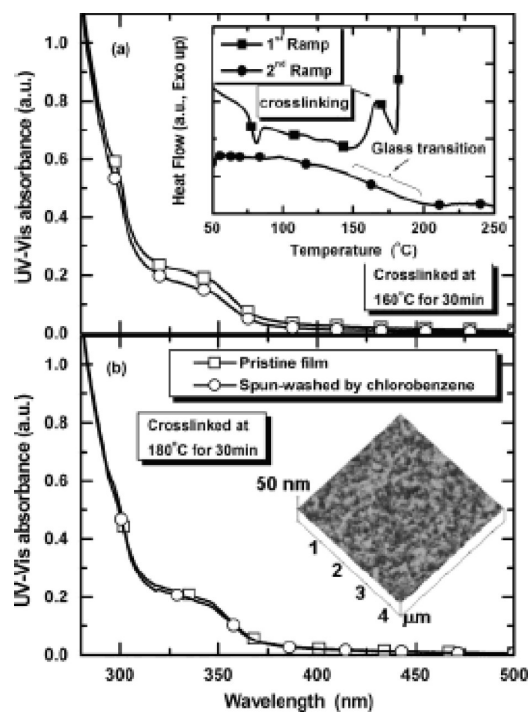


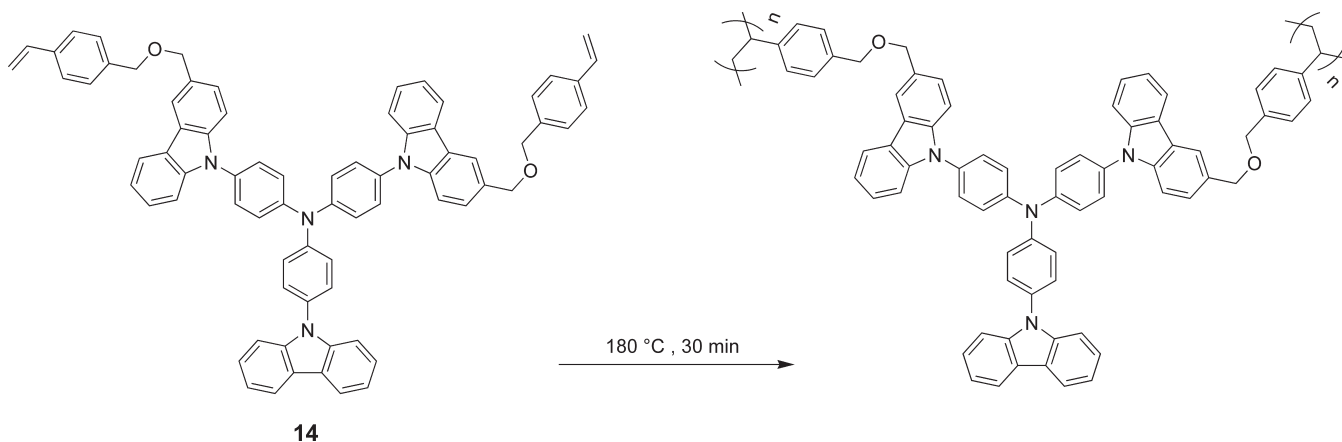
Figure 11. (a) Pre- and postwashing UV-vis of **14** cross-linked at 160 °C; inset shows DSC of (1st ramp) non-cross-linked and (2nd ramp) cross-linked **14**. (b) Pre- and postwashing UV-vis of **14** cross-linked at 180 °C; inset shows AFM post-cross-linking. Reproduced with permission from ref 33. Copyright Wiley-VCH Verlag GmbH & Co. KGaA.

hole injection into the emissive layer due to the ionization potential (IP) of this material lying between that of

Table 1. Data for OLEDs with Various Thicknesses of **14** (Scheme 5) Used As Hole-Transport Layer

	no hole-transport material	thickness of 14		
		15 nm	25 nm	34 nm
device no.	1	2	3	4
max η_{ext} (%)	2.07	4.01	5.85	5.2
power efficiency @ 800 cd/m ² (lm/W)	2.08	4.56	5.59	3.74

Scheme 5. Cross-Linking of a Styrene-Functionalized Tris(Carbazolyl) Triphenylamine Derivative



PEDOT-PSS and PVK, and to electron and/or exciton blocking. No devices were reported that would enable comparison of the performance of cross-linked and non-cross-linked **14** and, therefore, permit one to ascertain the effects on the functional transport groups of the thermal processing needed for cross-linking.

Another paper by Jen and co-workers³⁵ was concerned with small-molecule styrene-functionalized bis(diarylamino)-biphenyl derivatives **15–19** (Figure 12). DSC showed broad exothermic events above 150 °C for all the styrene-functionalized compounds with no additional exothermic events on second heating cycles. Films of the materials were cross-linked at 170 °C for 30 min and demonstrated good resistance to washing with chlorobenzene (annealing at 150 °C led to only ca. 85% resistance). The monofunctional **15** was, as expected, only polymerized and did not cross-link. AFM of the cross-linked thin films showed them to be smooth and free of defects with root-mean-square roughness values below 1 nm. Devices were fabricated with the following architecture: ITO/PEDOT:PSS/cross-linked-**16–19**/**4**/CsF/Al, where **4** acts as the electron-transport and emissive layer. Table 2 summarizes the devices and their performances. The results showed that the use of the cross-linked hole-transport materials improved device performance relative to a device with no such layer. As with their earlier work on **14** (see above), this was attributed to enhanced hole injection into the emissive layer and to exciton and/or electron blocking. Use of a higher cross-linking temperature of 230 °C led to poorer performance, which the authors attributed to degradation of the PEDOT-PSS. Again, this work demonstrates that a cross-linked hole-transport interlayer can facilitate solution processing of all the active layers of the device, the resulting device architecture leading to enhanced device performance while

employing a lower temperature cross-linking step relative to that required for some other cross-linking chemistries (e.g., BCB and TVFE thermal approaches, see below).

In 2009, Fréchet and co-workers³⁶ reported the development of cross-linkable bis(styrene)-functionalized heteroleptic iridium complexes **20–23** (Figure 13). DSC showed a broad exothermic event around 145 °C associated with the cross-linking event, no additional exothermic events being seen in a second heating, with only T_g events observed. The authors studied these emitters as hole-transport and electron-blocking materials, as well as emissive layers. Scheme 6 summarizes the cross-linking of these materials from compounds **20–23**. For hole-transport/electron-blocking applications, compound **20** (PPZ complex) was deposited and cross-linked. Blends of **20** with **21–23** (DFPPY, TPY, and PQ complexes) were used to achieve different colored emissive materials (in 90:10 wt % ratios of 1:2,3, or 4). These cross-linked films were evaluated for solvent resistance via UV-vis by monitoring absorption changes after washing films with chlorobenzene; 15 min was insufficient to fully insolubilize the layer, while 30 min proved adequate. Luminescence data for the materials before and after cross-linking showed no significant changes. AFM showed that smooth films were obtained from these materials. Compound **20** was studied as a cross-linkable hole-transport/electron-blocking layer in three types of devices: (I) ITO/EML/LiF/Al, (II) ITO/**24**/EML/LiF/Al, and (III) ITO/**24**/EML/Cs₂CO₃/Al {EML is a block copolymer host containing triphenylamine and oxadiazole moieties doped with a green-emitting Ir complex}. Films of compound **20** were deposited by spin-casting from chlorobenzene and cross-linked at 180 °C for 30 min to obtain cross-linked compound **24**. The results showed a near doubling of the device EQE with the introduction of the cross-linked layer of compound **24**. Improved hole

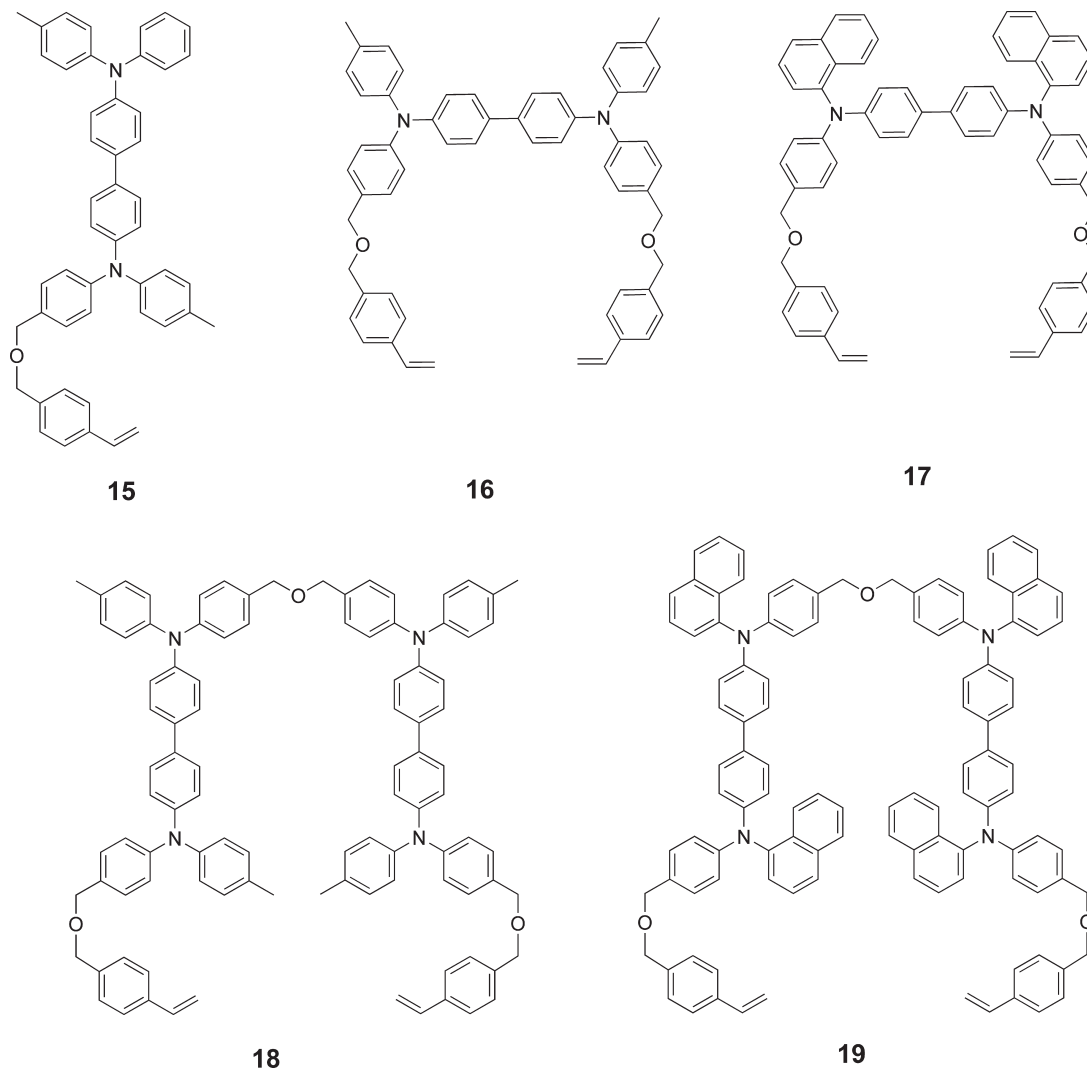


Figure 12. Cross-linkable styrene-functionalized bis(diarylamino)biphenyl derivatives.

Table 2. Data for OLEDs Using Styrene-Functionalized Bis(diarylamino)biphenyl Hole-Transport Materials

material	EQE (%)	luminance efficiency (cd/A)
none	0.72	2.42
16	1.78	6.29
17	2.92	9.45
18	2.15	7.56
19	3.2	10.8
20^a	0.99	3.51

^a cross-linked at 230 °C for 30 min; all others 180 °C for 30 min.

injection into EML and electron blocking by **24** were thought to be responsible for these improved properties. Cross-linked blends of **20** and **21–23** were evaluated as emitters in devices with the architecture: ITO/**24/25–27**/ETL/LiF/Al {ETL is a homopolymer of an oxadiazole-based material}. The devices represent good examples of fully solution-processed multilayer OLEDs. A near-white device in which the red-emitting material was doped into the blue-emitting host was also fabricated. For these all solution-processed devices, maximum efficiencies above 2% were reported, albeit with relatively low brightnesses

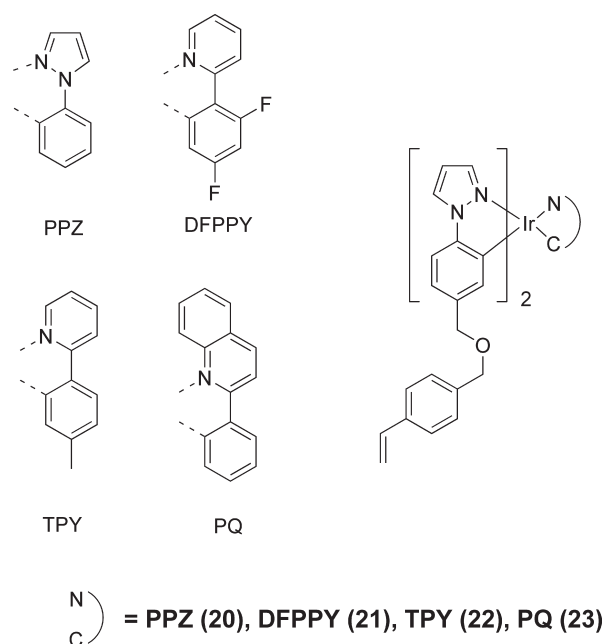


Figure 13. Cross-linkable phosphorescent emitters.

Scheme 6. Cross-Linking of Styrene-Functionalized Iridium Complexes

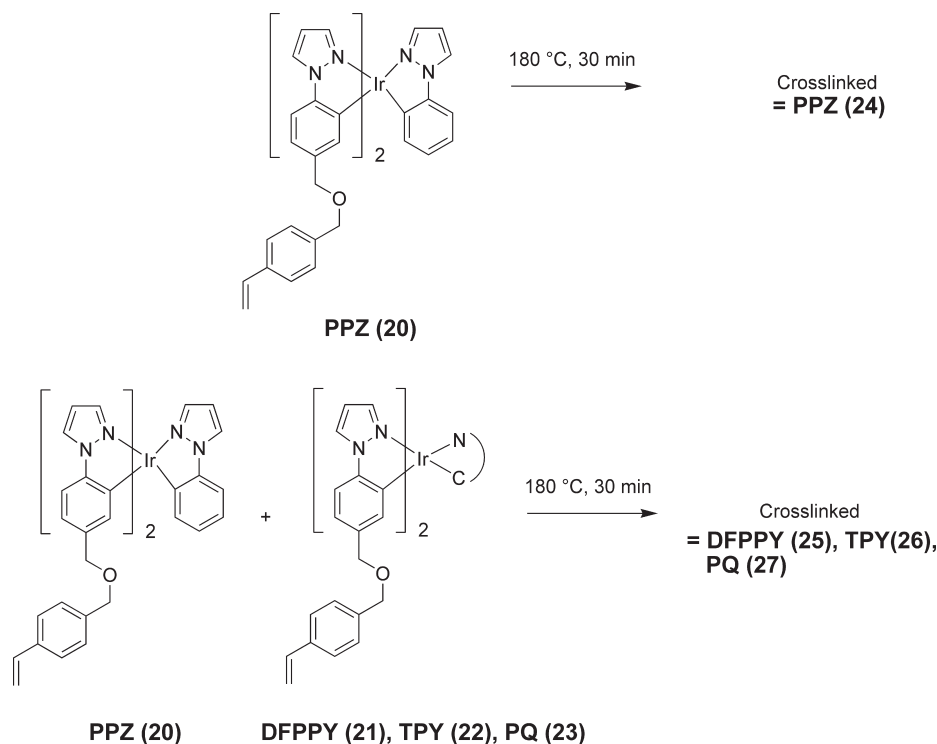


Table 3. Device Results for OLEDs Based on Cross-Linked Iridium Complexes

device ^a	max EQE (%)	brightness (cd/m ²)
I	5	225
II	9.8	125
III	9.2	145

^a See text for architectures.

(up to 400 cd/m² at high driving voltages of 20–25 V) (see Table 3). The low brightness and efficiencies were attributed by the authors to the poor electron transport by the complexes, leading to an imbalance of charge in the emissive layer.

Acrylates. Acrylates are another class of monomer readily polymerized by a radical mechanism. The polymerization is generally carried out using thermal or photochemical activation of a radical initiator. Accordingly, a molecule functionalized with two or more acrylate groups can give a cross-linked network when polymerized.

Bacher et al.³⁷ reported the synthesis of a series of acrylate-functionalized hexaalkoxytriphenylenes in 1999 (Figure 14). The monoacrylate-functionalized compound **28** was photopolymerized to give a soluble linear polymer with a photoradical initiator (2,4,6-trimethylbenzoyldiphenylphosphine oxide, which absorbs strongly in the 350–400 nm range) under UV exposure at 130 °C (under an inert atmosphere) as a test of photopolymerization conditions. The di- and triacrylates were subsequently used to form cross-linked polymer networks. IR spectroscopy was used to monitor functional group changes in the films before and after cross-linking. UV–vis spectra of the polymers showed little change following the UV irradiation, while the absence of significant changes following washing with dichloromethane indicated successful insolubilization

by the cross-linking. UV cross-linking in combination with a photomask was used for photopatterning of the polymer network and the patterned material was characterized by surface profiling and scanning electron microscopy. The materials were subsequently tested in OLEDs having the architecture: ITO/photopolymerized **28–33**/Alq₃/Al. Devices fabricated based on photopolymerization/cross-linking of films of the hole-transport monomers **28–33** showed device brightnesses (at 10 mA/cm²) decreasing in the order **28** (90 cd/m²) > **29** (67 cd/m²) > **30** (78 cd/m²) > **31** (13 cd/m²) > **32** (8 cd/m²) > **33** (3 cd/m²). Interestingly, the device based on a photopolymerized film of polymer **28** showed a brightness ca. 10 times lower than an equivalent device based on film spin-coated from a sample of poly-**28** synthesized in solution.³⁸

In 2006, work on a cross-linkable derivative of tris(8-hydroxyquinolino)aluminum (Alq₃) was published by Du et al. (Scheme 7),³⁹ with the aim of inhibiting the crystallization that has been observed for vacuum-processed Alq₃ layers. Cross-linking was performed by either UV irradiation using a photoinitiator or thermally (150 °C for 15 min), to give either the homopolymer (**34**) or a copolymer with *N*-vinylcarbazole (**35**). To determine whether the process was successful in forming a cross-linked polymer network, DSC and TGA data were obtained. DSC data for the UV-irradiated films did not show the Alq₃ glass transition, typically observed at 120 °C, and this was taken as evidence of the formation of the polymer network. TGA data showed increased thermal stability at high temperatures versus a linear chain Alq₃ polymer. OLED devices were fabricated with the architecture: ITO/PEDOT-PSS/**34** or **35**/LiF/Al. When comparing the homo- and copolymers, the efficiencies showed that

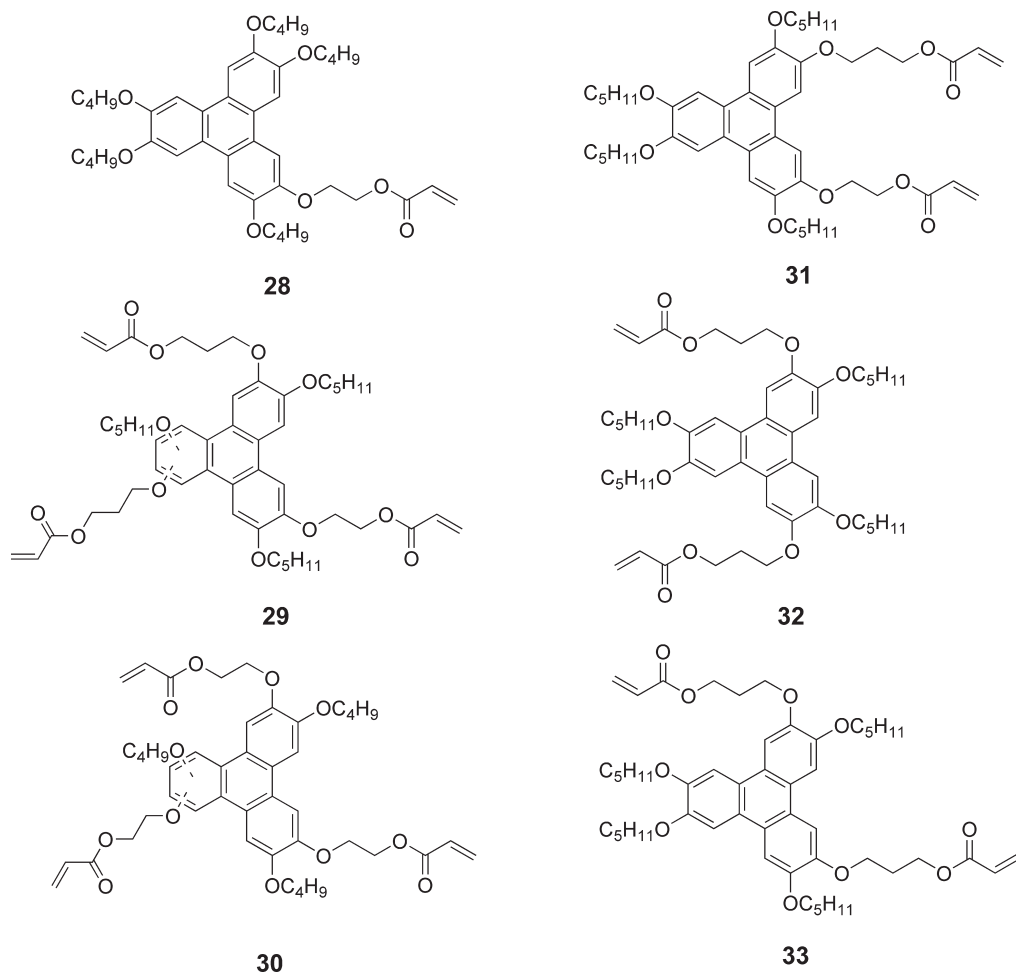


Figure 14. Hexaalkoxytriphenylenes (**28**–**33**) bearing one, two, or three polymerizable acrylate groups.

the co- polymer with a 10:1 ratio of Alq₃ to carbazole was the most efficient (approximately 4–5 times higher than the homopolymer).

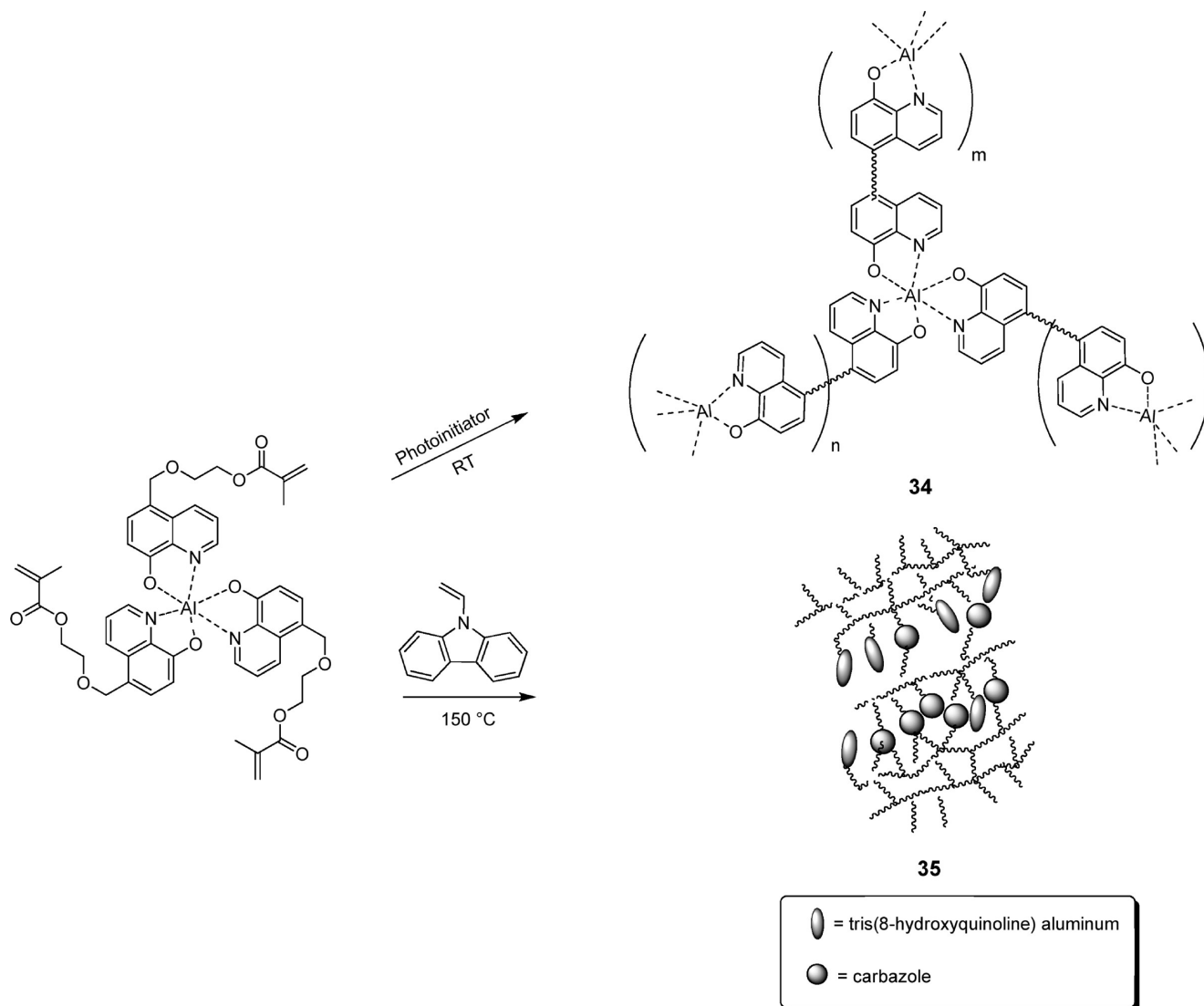
Trifluorovinylethers. The trifluorovinylether (TFVE) group is known to undergo a thermally activated 2 + 2 cycloaddition to form a hexafluorocyclobutane moiety at temperatures of ca. 200 °C (Scheme 8).⁴⁰ The process is reported to occur via diradical intermediate that subsequently ring closes; head-to-head cycloaddition predominates.⁴¹ This reaction typically proceeds with minimal side reactions and can be carried out in the presence of a wide range of functional groups, making this an attractive cross-linking strategy for organic electronics application, the major consideration being the thermal stability of the active materials at the reaction temperature. However, because this is a dimerization, rather than a polymerization, at least three TFVE groups must be incorporated into small molecules in order to ensure cross-linking; this situation can be contrasted to groups such as styrene and acrylate discussed above.

In 2006, Niu et al.⁴² reported on the use of TFVEs to cross-link a hole-transport polymer in which styrene monomers with TFVE side chains were copolymerized with monomers with bis(diarylamino)biphenyl side chains (Figure 15). **36** could be thermally cross-linked at 235 °C for 40 min and was used, along with another TFVE-functionalized material,

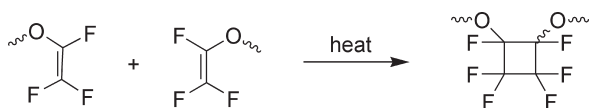
a tris(trifluorovinylethyl)-functionalized tris(carbazolyl) triphenylamine small molecule (**37**, Figure 15) in an OLED with the architecture: ITO/**36**(20 nm)/**37**/EML/TPBI/Al {EML = solution processed emissive layer composed of an iridium-based phosphor in a blend of PVK and TPBI}. Thus, the use of TFVE cross-linking permits fabrication of an OLED with three solution-processed layers, the two cross-linked layers acting as a redox cascade for hole injection from ITO into the emissive layer. The device showed an EQE of 3%, whereas an analogous device omitting the **37** material demonstrated a much lower EQE of 1.24%, which was attributed to a large barrier for hole injection from **36** into the emissive layer.

Another tris(trifluorovinylether)-functionalized hole-transport small molecule (Figure 16) was reported by Lim et al.⁴³ in 2006, with the intention of developing an alternative hole-transport/hole-injection material to PEDOT-PSS. TGA indicated good thermal stability with respect to weight loss, whereas a large exothermic peak was observed in the DSC at 230 °C. Complete insolubilization in chlorobenzene (as revealed by UV–vis) required 2 h of heating which may be rather long for a processing step for commercial applications and increases the probability of thermal damage to the active materials. Cross-linking was carried out heating to 230 °C for 2 h. AFM images of these cross-linked films showed a smooth

Scheme 7. Cross-Linkable Tris(8-hydroxyquinolino)aluminum Derivative and Its Homopolymerization or Copolymerization with *N*-Vinylcarbazole



Scheme 8. Thermal 2 + 2 Cycloaddition of a Trifluorovinyl Ether



surface with a root-mean-square roughness smaller than that of PEDOT-PSS (0.47 nm vs 1.15 nm)). The polymer HTL was tested in an OLED with the architecture: ITO/ **38**/PFO/Ba/Al {PFO = poly-2,7-(9,9-dioctylfluorene)} and compared to an equivalent device with PEDOT-PSS in place of the cross-linked material. The devices had similar EL spectra. The device with the cross-linkable layer showed a higher turn-on voltage than that with PEDOT-PSS, but the luminance and luminance efficiency (0.132 cd/A vs 0.091 cd/A) were improved. The study clearly shows the successful employment of the TFVE cross-linking groups in small-molecule based HTL layers, but the relatively long time at high temperature required for cross-linking could prove problematic if extended to other active materials (although higher

numbers of TFVE groups per molecule could perhaps help in this regard).

Benzocyclobutenes. The benzocyclobutene (BCB) group is another example of a moiety that undergoes a thermally activated dimerization, typically at 200 °C or above, in this case forming a dibenzocyclooctadiene ring,² which is formed by scission of one of the cyclobutene C–C bonds, followed by an irreversible cycloaddition (Scheme 9).⁴⁴ The Fréchet group¹ in 2007 reported a polystyrene with bis-(diarylamino)biphenyl and cross-linkable benzocyclobutene side groups, **39** (Figure 17). The cross-linking of **39** (m:n = ca. 9:1) was initiated by heating between 180 and 250 °C (it was unreactive at temperatures below 150 °C); this led to the irreversible formation of dibenzocyclooctadiene rings. The cross-linked polymer was reported to possess good stability toward ambient atmosphere, moisture, and light. The results of DSC, UV–vis, and AFM studies of the material are summarized in Figure 18. The UV–vis spectra illustrate the effect of 2 h vs 4 h of thermal annealing on the solubility in chloroform; it was evident that 2 h is insufficient to fully insolubilize the film. AFM studies showed

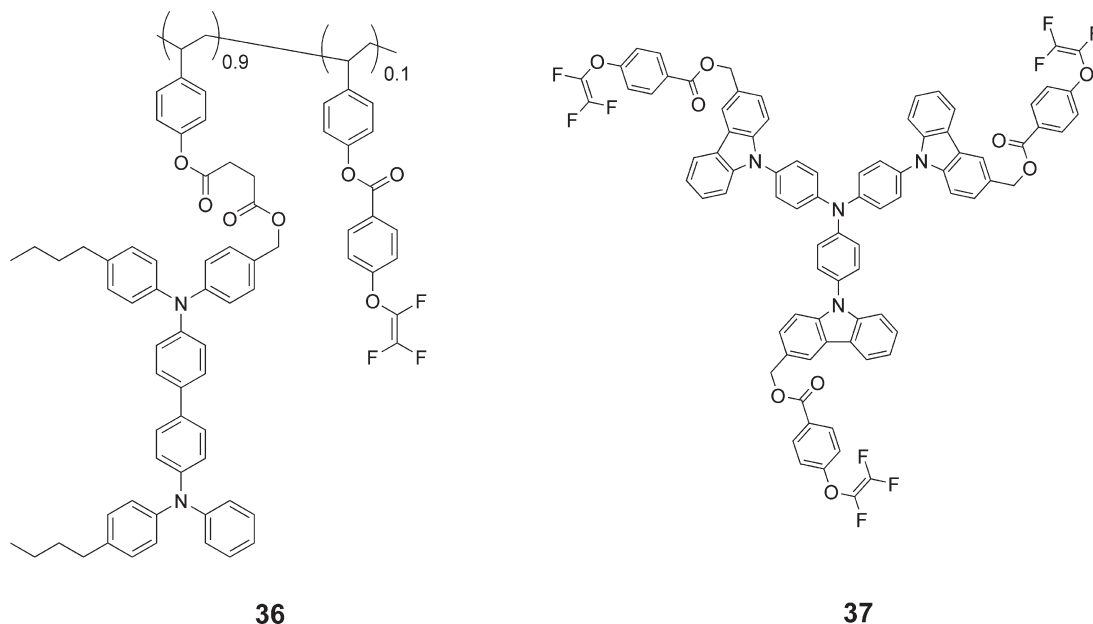


Figure 15. Hole-transport materials with trifluorovinylether cross-linking groups.

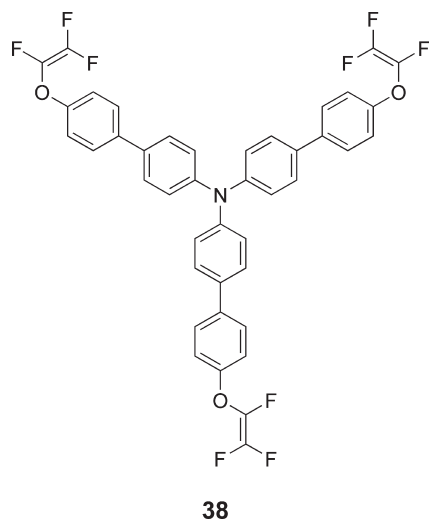


Figure 16. Tris(trifluorovinyl)-functionalized triphenylamine.

that the cross-linked polymer film produced was smooth. OLED devices were fabricated using the general architecture ITO/**39**/Alq₃/LiF/Al, both with and without cross-linking **39**, or a small molecule TPD equivalent device for comparative purposes. Testing of all OLED devices showed emission was from the Alq₃ emissive layer exclusively. EQE values showed little difference between the cross-linked and uncross-linked **39** devices (both ca. 0.7%), but both of these devices had slightly lower efficiencies compared to the small-molecule TPD device (ca. 0.89% efficiency). The authors also fabricated a trilayer OLED with the architecture: ITO/cross-linked-**39**/EML/BCP/LiF/Al {EML is a bipolar polymer with oxadiazole and triphenylamine side chains doped with an Ir phosphor; BCP = bathocuproine}. A device without any hole-transport layer was also fabricated for comparison purposes. The device with the cross-linked hole-transport layer had a lower turn-on voltage and possessed a higher current density at low voltages. At higher voltages,

though, the current density was lower for the cross-linked device. The EQE increased from 6.4% to 10.4% following the introduction of the cross-linked hole-transport material; this was attributed to better exciton confinement and movement of the recombination zone toward the center of the device. This work demonstrates both that the thermal cross-linking of BCB groups does not adversely affect device performance (in the Alq₃ devices) and that BCB cross-linking permits fabrication of more efficient devices incorporating two solution-processed layers (in the phosphorescent devices). The prolonged heating apparently required to effect cross-linking may, however, prove to be a limitation of the use of BCB with application to other OLED materials.

Cinnamates and Chalcones. Cinnamates and chalcones can react via a [2 + 2] cycloaddition (shown in Scheme 10 for a cinnamate) when exposed to UV irradiation and have been used widely as cross-linkers for polymers for some time.^{45,46} Cinnamates and chalcones absorb at ca. 290 and ca. 345 nm, respectively and so moderate transparency of the active material at these wavelengths is desirable in order to allow light to reach the cross-linking groups and to minimize the possibility of photodamage to the active material. As with the thermal reactions of TFVE and BCB groups, this reaction is a dimerization and so at least three cinnamates or chalcones per molecule are required to achieve cross-linking. Thus far, however, the use of these reactions in the context OLEDs has been restricted to side-chain polymers.

An early demonstration of cross-linking to produce robust films for OLED applications involved cinnamate groups and was reported by Li et al.⁴⁷ in 1997: a poly-(methacrylate) ter-polymer (**40**, Scheme 11) was synthesized with distyrylbenzene-, oxadiazole-, and cinnamate-containing side chains, with the polymer composition being controlled by changing the monomer feed ratios. Pin-hole free films were readily deposited by spin-coating or drop-casting and could be cross-linked using UV

Scheme 9. Benzocyclobutene thermally initiated cross-linking

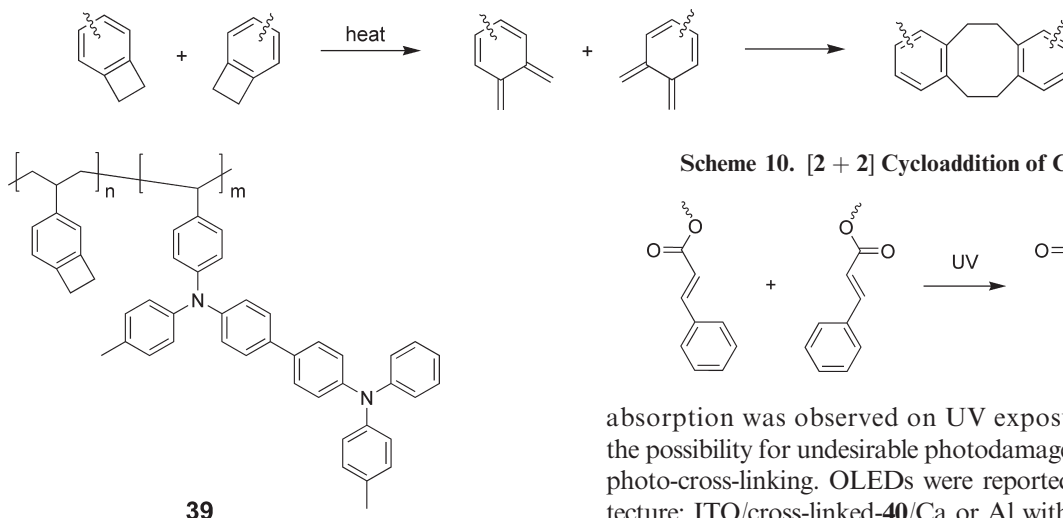


Figure 17. Benzocyclobutene-bis(diarylamino)biphenyl copolymer.

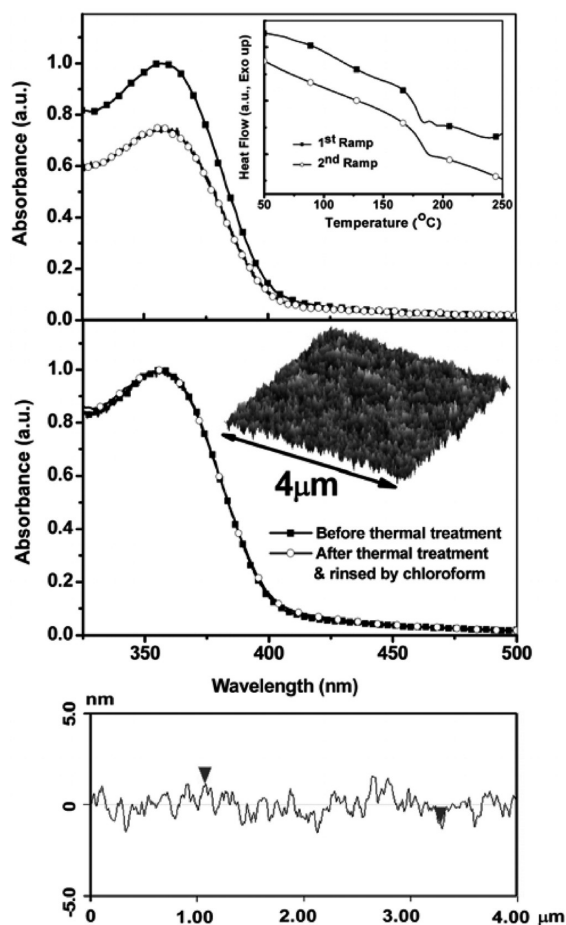
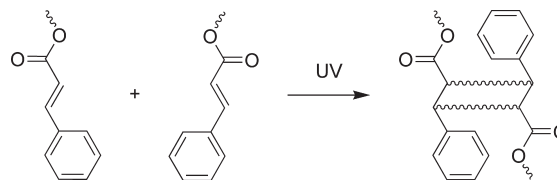


Figure 18. UV-vis spectra of **39** before (dark squares) and after washing with chloroform following cross-linking (open circles) for 2 h (top) and 4 h (bottom); top inset shows DSC of **39** and bottom shows an AFM image of the cross-linked film. Reproduced with permission from ref 1. Copyright 2007 American Chemical Society.

exposure (in air) for 10 min or longer. DSC showed an increase in the glass-transition temperature from 107 to 154 °C on cross-linking. A decrease in the distyrylbenzene absorption at 394 nm as well as the cinnamate

Scheme 10. [2 + 2] Cycloaddition of Cinnamates



absorption was observed on UV exposure, illustrating the possibility for undesirable photodamage when using UV photo-cross-linking. OLEDs were reported with the architecture: ITO/cross-linked-**40**/Ca or Al with an efficiency of 0.1% for the Ca device.

Zhang et al.⁴⁸ used a copolymer of methacrylate monomers with side chains incorporating bis(diarylamino)-biphenyl and cinnamate (**41**) or chalcone (**42**) groups (see Figure 19). UV-vis data following different UV exposure times showed decreases in overall near-UV absorption for copolymers **41** and **42**; this was attributed to the cycloaddition reaction. For a homopolymer containing only the hole-transport monomer, no change in absorption was observed, which suggested this group was stable against photodecomposition. Insolubilization of the copolymers was demonstrated by UV-vis spectra of the photopolymerized films both before and after tetrahydrofuran washing. To test the effect of cross-linking on OLED device performance, OLEDs were fabricated with the architecture ITO/**41** or **42**/Alq₃/Mg with or without cross-linking. When tested, the devices were shown to be less efficient when cross-linked, despite the UV-vis evidence that the hole-transport groups were largely unchanged. This was consistent with earlier work in which triarylamine-functionalized polynorbornenes were found to undergo UV-promoted cross-linking (the mechanism of which was unclear) that was accompanied by a marked decrease in device performance.⁴⁹

An additional study of similar cross-linkable copolymers (**43**–**46**, Figure 20) was reported in 2003;⁵⁰ this focused on a range of substituted hole-transport derivatives with a slightly different linker group and demonstrated both photopatterning of the polymers (Figure 21) and that OLEDs could be fabricated with similar performance to non-cross-linked devices. AFM was used to show that the cross-linked films showed little change after annealing at 160 °C, while vapor-deposited films of TPD changed significantly at only 80 °C. OLED devices were fabricated with the general architecture: ITO/**43**–**46**/Alq₃/Mg:Ag. The EQEs of **45**-based devices were studied as a function of UV energy exposure per unit of area (see Figure 22); the EQE was stable up to a 25 mJ/cm² dose of 350 nm light, but decreased beyond that, demonstrating that triarylamine-based systems can be relatively stable under limited UV exposure. Cross-linking was also exploited to fabricate devices with two solution-processed

Scheme 11. Cross-Linking of a Cinnamate-distyrylbenzene-oxadiazole Copolymer

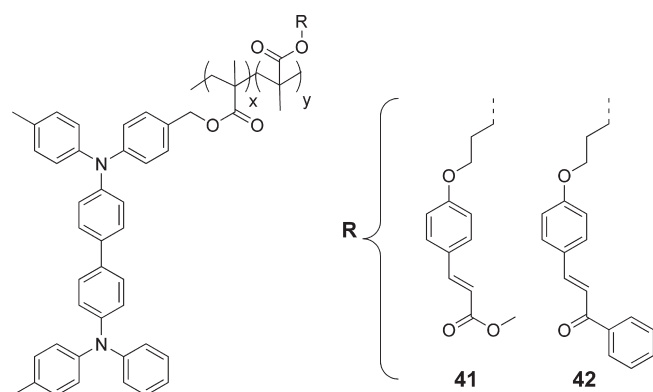
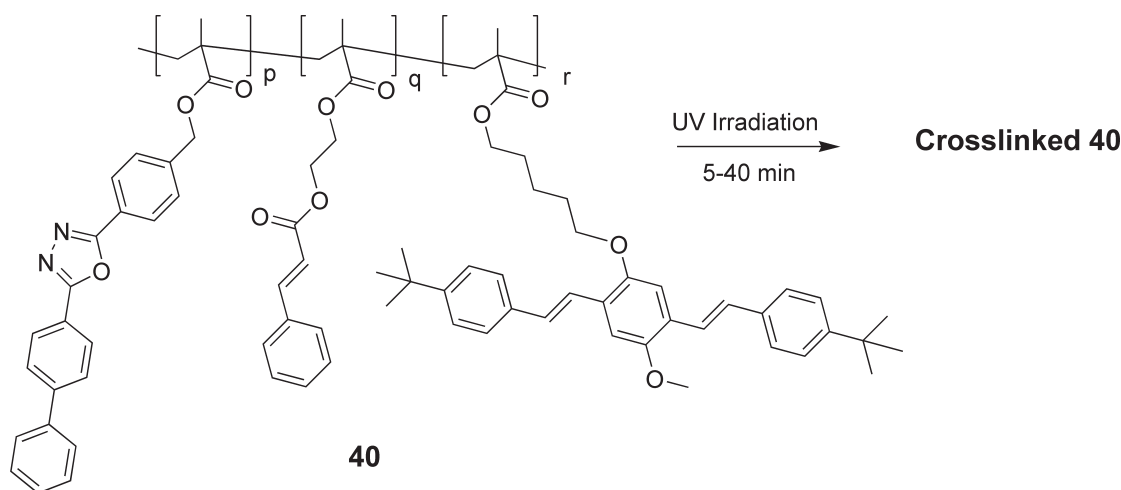
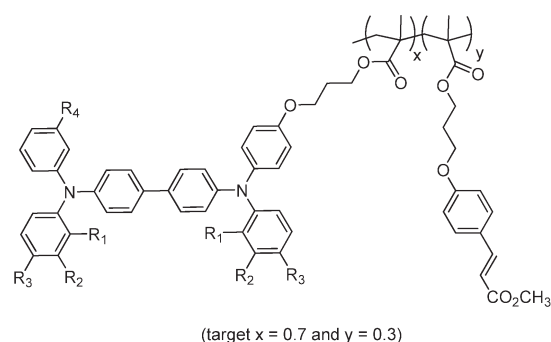


Figure 19. Cross-linkable copolymers of bis(diarylamino)biphenyl and cinnamate or chalcone methacrylates.

cross-linked layers: ITO/44/(43 or 45)/Alq₃/Mg:Ag. These devices showed increased EQE relative to devices with a single cross-linked hole-transport layer; this was attributed to more facile stepwise injection of holes from ITO into the lower-IP polymer, the higher-IP polymer, and finally into Alq₃ in the trilayer devices, in contrast to a two-step process in a bilayer device where one of the two barriers is considerably larger. The lifetimes of OLEDs with a single cross-linked hole-transport layer were studied. For 43–46, the device half-lifetimes were 681, 1575, 1849, and 840 s when cross-linked, while a value of 1550 s was found for a device based on un-cross-linked 44. Although these half-lifetimes for all these devices with solution-processed hole-transport layers are much less than that for an analogous control device based on vapor-deposited TPD (36000 s), the data clearly show that, at least for these systems, the UV cross-linking process itself (when optimized) does not adversely affect OLED lifetime. The successful identification of conditions under which these polymers can be cross-linked without significant impacts on device performance (relative to non-cross-linked analogues) has led to subsequent use of cross-linked 45 in OLEDs as a hole-transport material onto which polymeric electron-transport⁵¹ or emissive^{52–54} layers are solution-processed.

Oxetanes. Oxetanes are strained four-membered cyclic ethers that can undergo cationic ring-opening



polymer	R1	R2	R3	R4
43	H	Me	H	H
44	H	H	OMe	Me
45	H	F	H	Me
46	F	H	F	Me

Figure 20. Methacrylate bis(diarylamino)biphenyl-cinnamate copolymers.

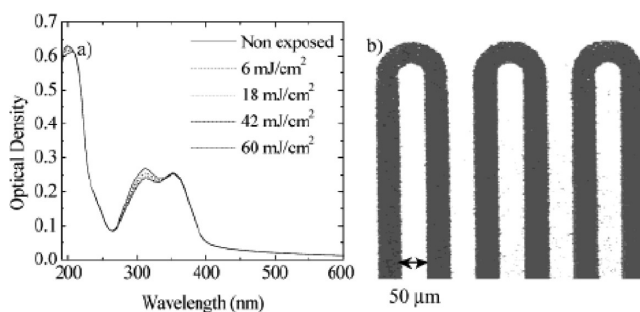


Figure 21. UV–vis spectra of 45 after different doses of UV irradiation and image of a photopatterned film of 44. Reproduced with permission from ref 50. Copyright 2003 American Chemical Society.

polymerization (CROP) to form linear polyethers.⁵⁵ Accordingly, a molecule functionalized with two or more oxetanes can be cross-linked when a suitable initiator of the cationic polymerization process is added (see Scheme 12). Often the process is initiated by the use of UV photoacid-generators such as diaryliodonium or triarylsulfonium salts. These photoacid-generators typically show strong absorptions in

the UV (e.g., 235 nm for Ph_3S^+ ,⁵⁶ although absorption maxima can be red-shifted through substitution⁵⁷), excitation of which leads to a bond cleavage and ultimately to the generation of a strong acid, but can also generate protons when sensitized (through an electron-transfer mechanism) by dyes with longer absorption wavelengths,^{57–59} thus potentially including active materials used in OLEDs. Potential advantages of this approach include the low shrinkage generally observed on oxetane polymerization and the relatively high polymerization rates,^{60–62} although heating is often used subsequent to photoinitiation to drive the polymerization toward completion, especially when the oxetane moieties are not particularly mobile at room temperature. Of course, for OLED applications, it is important that the active materials involved are not themselves sensitive to strong Brønsted acids. In addition, protons or oxonium species are likely to remain in the material following CROP; in particular, protons may then migrate to other layers of the device under the influence of the electric field used

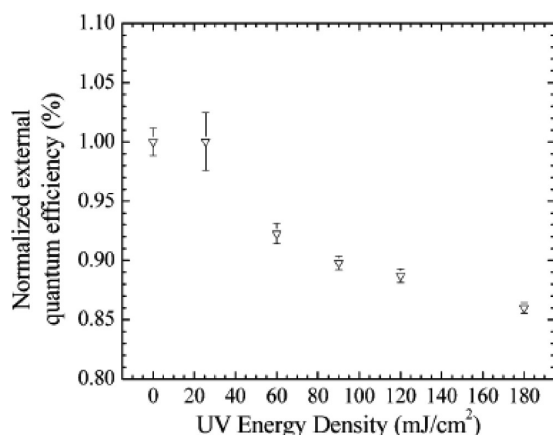


Figure 22. UV dosage effects on the EQE of OLEDs in which **45** is the hole-transport layer. Reproduced with permission from ref 50. Copyright 2003 American Chemical Society.

for device operation. In some cases, bases and nucleophiles have been used to neutralize these species, but this of course raises the possibility of incorporating additional impurities into the films. Nevertheless, a variety of OLEDs, including some with high efficiencies, have been demonstrated based on oxetanes.

Early work on oxetanes for cross-linking was reported in 1999 by Bayerl et al.⁶¹ To show the oxetane moiety could be successfully employed to cross-link a layer in an OLED device, they synthesized bis(diarylamino)biphenyl modified with either short or extended oxetane functionalities (**47** and **48**, Figure 23). Films of **47** or **48** were deposited on ITO along with 1 wt % of a photoacid—4-(thiophenoxyphenyl)-diphenylsulfonium hexafluoroantimonate—and cross-linked by UV exposure (1 min at 302 nm). The films became insoluble and DSC showed disappearance of the glass-transition events observed for the monomers. To establish the effect cross-linking had on device performance, researchers fabricated two devices with polymer **47** with and without cross-linking (architecture: ITO/**47**/Al). The cross-linked device showed a marked increase in current maximum (15 times greater) compared to the non-cross-linked device. A second type of device containing an additional emissive layer spin-coated onto cross-linked **47** was fabricated (architecture ITO/cross-linked-**47**/EML/Ca {electron-transport/emissive layer, EML = blend of poly(α -methylstyrene, PBD, and perylene}) and emitted blue light at 2000 cd/m² under continuous operation.

Nuyken et al.¹⁷ reported a range of oxetane-functionalized diamine derivatives in 2002 (Figure 24). After UV cross-linking using a sulfonium salt photoinitiator the films were found to be resistant solvent by inspection of the UV-vis absorption spectra. OLED test devices (architecture: ITO/**49** or **50**/Ca) were demonstrated using these cross-linked materials as the single active layer. Another approach examined was the synthesis of

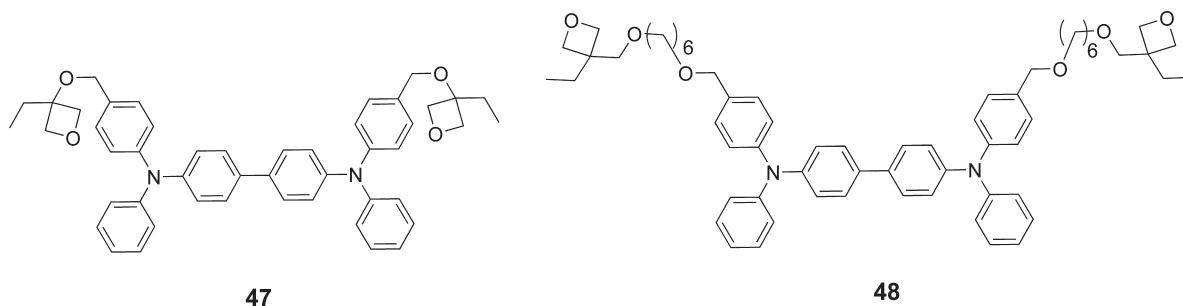
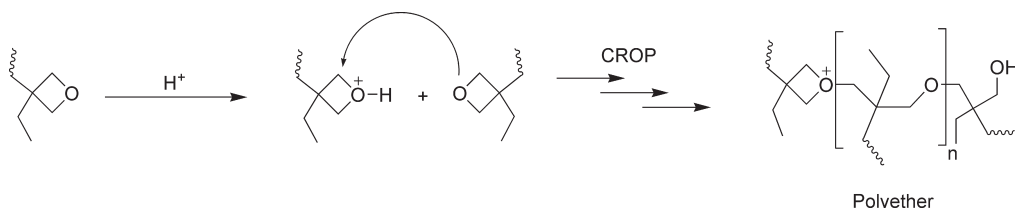


Figure 23. Oxetane-functionalized bis(diarylamino)biphenyl derivatives studied by Bayerl et al.

Scheme 12. Cationic Polymerization of Oxetanes



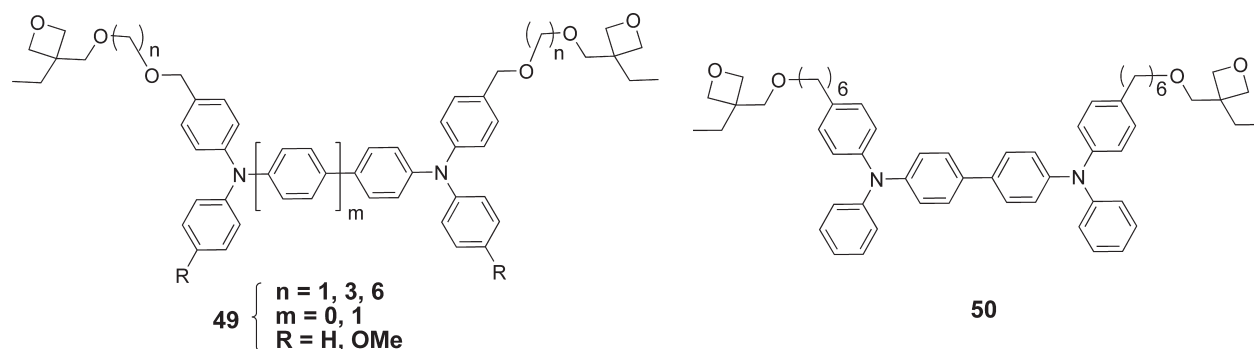


Figure 24. Oxetane-functionalized bis(diarylamino)oligophenylene derivatives studied by Nuyken et al.

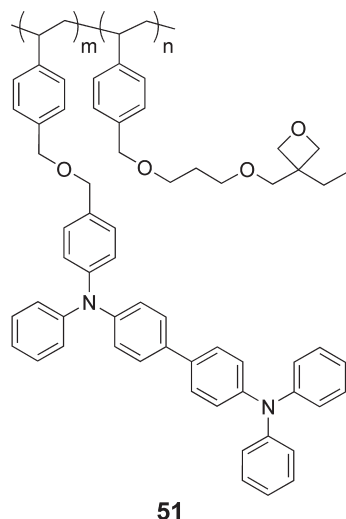


Figure 25. Oxetane-bis(diarylamino)biphenyl copolymer.

copolymers containing hole-transport and oxetane groups as side-chain functionalities (Figure 25). Introduction of the oxetane comonomer was reported to adversely affect the hole-transport properties of the polymer; this was attributed to dilution of the transport functionality by the electronically inert cross-linking comonomer.

The oxetane cross-linking functionality was integrated into a series of conjugated polymers that were shown to be patternable by photomasking, as reported in 2003, by Meerholz and co-workers (Scheme 13).⁶³ Arylene building blocks were incorporated in different feed ratios to afford polymers with a variety of emission colors as summarized in Table 4. Here the oxetane groups were used to cross-link multiple layers in a multicolor OLED in which the active layers were processed entirely through spin-coating. All polymers except **55** contained the oxetane functionality. Photopolymerization was achieved by exposing the polymers (**52–54**) to UV (3 s at 302 nm) in the presence of a photoacid generator (4-[(2-hydroxytetradecyl)-oxyl]-phenyl}-phenyliodonium hexafluoroantimonate). IR measurements showed the disappearance of the oxetane groups after UV irradiation; the chain ends were reported to be oxonium cations that required treatment with several bases or nucleophiles (except for tetrahydrofuran, these were not specified) to neutralize the cationic charges. Evaluation of the PL and EL

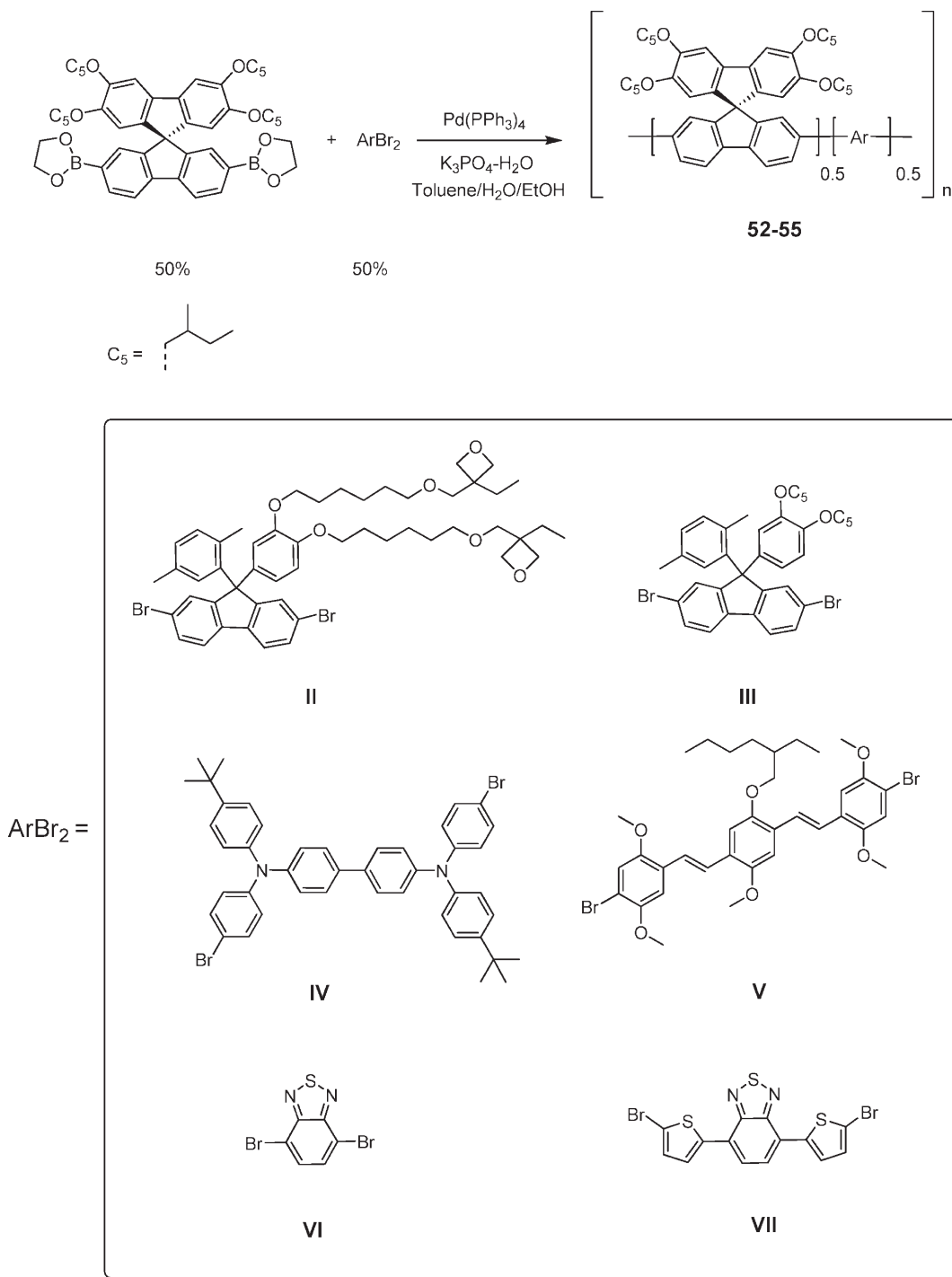
Table 4. Composition of Oxetane-Functionalized Conjugated Polymers (See Scheme 13)

	color-emitting polymers			
	52 (X-blue)	53 (X-green)	54 (X-red)	55 (blue)
I moiety (mol %)	50	50	50	50
II	25	25	25	
III	15			
IV	10	10	10	10
V		15		
VI			10	
VII			5	
η_{\max} (pristine) (cd/A)	2.9	7	1	3
η_{\max} (cross-linked) (cd/A)	3	6.5	1.1	n.a.

spectra showed no effect from cross-linking. OLED devices with an architecture: ITO/PEDOT/EL polymer (**52–55**)/Ca/Ag were fabricated. Compound **55** was used for a non-cross-linkable control device. Initial devices were not cross-linked and all devices **52–55** showed good efficiencies that were comparable to the best reported values at that time for fluorescent OLEDs, suggesting that the presence of oxetanes has little effect on the hole- or electron-transport properties of the active functionalities or the emission of the polymers. When cross-linked, devices based on **52–54** all demonstrated high efficiencies (at high luminance) and resisted breakdown at high current densities than non-cross-linked devices.

Another study of the oxetane-functionalized bis(diarylamino)biphenyl derivative **50** (Figure 24) was published by Bacher et al.⁶⁴ The photopolymerization process (in the presence of a photoacid generator) was monitored using IR spectroscopy as a function of different UV exposure times: the intensities of polyether peaks (at 1175 and 1020 cm^{-1}) increased and that of oxetane (980 cm^{-1}) decreased (Figure 26). Photopatterning by UV irradiation through a shadow mask required heating to ensure the mobility of the oxetane groups during the cross-linking process. After removal of the non-cross-linked material by washing with THF the patterned surface was examined by AFM to reveal a good replica of the pattern of the shadow mask (Figure 27).

A side-chain approach was explored by Bacher et al.⁶⁵ based on various types of cross-linkable copolymer of monomers containing hole-transporting diamines and oxetanes (Figure 28). DSC showed the polymers to have glass transitions below 100 °C which proved important

Scheme 13. Cross-Linkable Copolymers Containing Bis(oxetane)-Functionalized Moiety (ArBr₂ = II) (Compositions of 52–55 are Defined in Table 4)

with respect to the photocross-linking process as will be discussed below. Films of the polymers were cross-linked in the presence of a photoacid generator (doped at 1 wt %) by exposure to UV light (10 s at 366 nm) with a curing step at 150 °C postirradiation, i.e., above the glass-transition temperature to increase the mobility of the oxetane groups. In the absence of the heating step, the viscosity limited the effective reaction of the oxetane groups. Simple OLEDs were fabricated with the architecture: ITO/**56–63**/Ag. A reference device was also prepared with the cross-linkable small-molecule diamine derivative **64** (Figure 29). The

copolymer devices had a higher turn-on voltage than the **64** device; this was attributed to the overall lower proportion of diamine to electronically inactive backbone and/or oxetane groups in the copolymers.

Meerholz and co-workers⁶⁶ studied **64** (see Figure 29), **65**, and **66** (Figure 30) as cross-linkable hole-transport layers onto which emissive/electron-transport layers composed of PVK, Ir phosphors, and oxadiazole-derivatives were solution-processed. Some of the devices showed very good performance, especially for solution-processed OLEDs. The best device (based on a green phosphor)

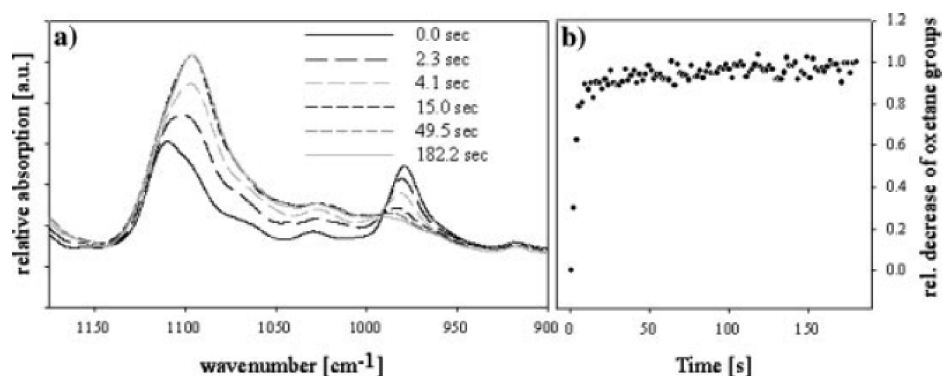


Figure 26. (a) Effect of UV exposure on the attenuated total reflectance IR spectra of a film of **50** and (b) data derived from IR data showing the decrease in the oxetane content with UV irradiation time. Reproduced with permission from ref 64. Copyright Wiley-VCH Verlag GmbH & Co. KGaA.

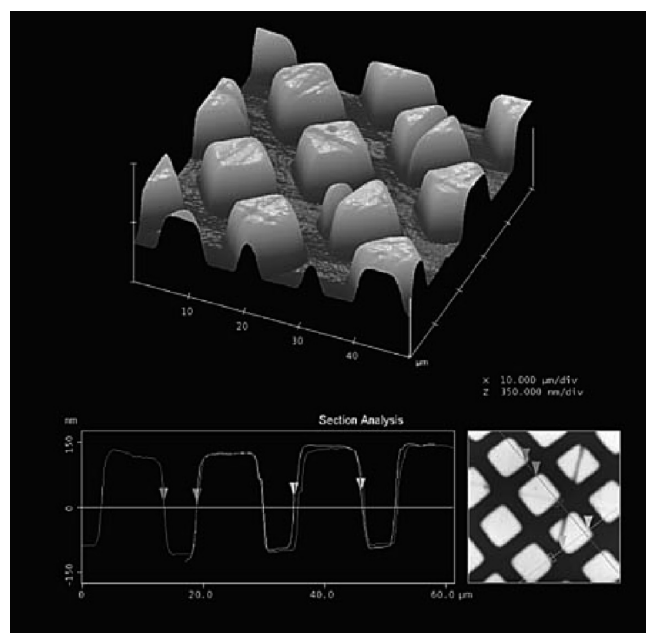
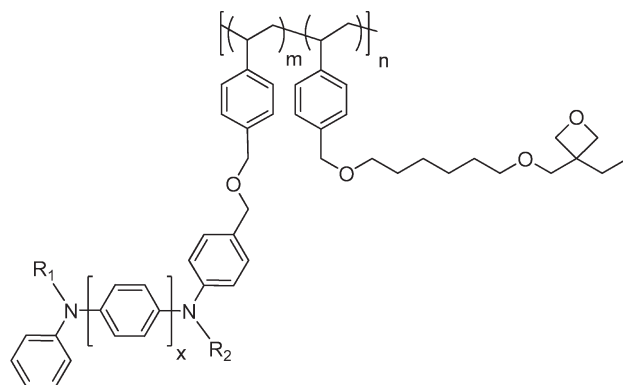


Figure 27. AFM image of a UV-patterned surface of **50**. Reproduced with permission from ref 64. Copyright Wiley-VCH Verlag GmbH & Co. KGaA.

showed a maximum EQE of 18.8% (depending on conditions) and at 100 cd/m² the power efficiency was calculated to be 50 lm/W, better than other green polymer-based devices at that time. This device used two cross-linked layers: a hole-injection layer consisting of cross-linked **66**, chemically p-doped with NOSbF₆, and a second layer of cross-linked **66**. A similar red device exhibited an EQE of 13%. Blue devices (not directly comparable because of different host materials) exhibited a lower EQE of 5.7%, attributed to poor triplet state confinement. In all cases, the device lifetimes were noted to be quite limited; however, the authors noted that this is a general problem with some of the PVK/oxadiazole host systems and so the cross-linking process is not necessarily implicated here.

An oxetane-functionalized phosphor, **67** (Figure 31), has also been used in multilayer cross-linked orange-emitting devices; the best performance was obtained from a device with the architecture: ITO/PEDOT-PSS/**66/64**/EML/ETL/CsF/Al.⁶⁷ Films of hole-transport

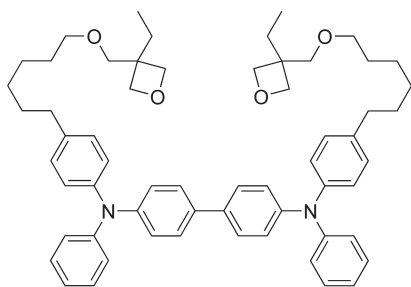


Name	x	R ₁	R ₂	(m:n)
56	1	Phenyl	Phenyl	(1:1)
57	1	Phenyl	Phenyl	(3:1)
58	2	Phenyl	Phenyl	(1:1)
59	2	Phenyl	Phenyl	(3:1)
60	2	1-Naphthyl	1-Naphthyl	(1:1)
61	2	1-Naphthyl	1-Naphthyl	(3:1)
62	2	1-Naphthyl	Phenyl	(1:1)
63	2	1-Naphthyl	Phenyl	(3:1)

Figure 28. Copolymers containing oxetane and bis(diarylamino)biphenyl or bis(diarylamino)benzene groups in the side chains.

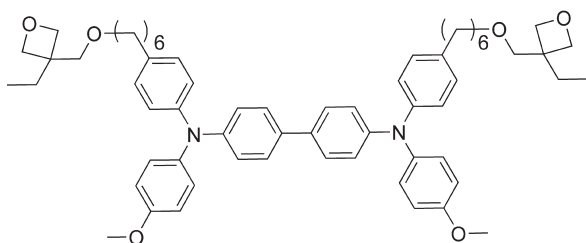
materials **66** and then **64**, containing 2.0 and 0.5 wt %, respectively, of 4-octyloxy-diphenyliodonium hexafluoroantimonate were successively deposited and cross-linked using UV irradiation (365 nm for 6s) with a postexposure bake (110 °C for 1 min). The EML was comprised of 81.7 wt % of **64**, 15 wt % of **67**, and 3.3 wt % of an initiator (4-octyloxy-diphenyliodonium-hexafluoroantimonate) and was also cross-linked by UV exposure (365 nm for 10 s) followed by a postexposure bake (150 °C for 15 min). At low phosphor loadings, there is incomplete energy transfer from **64** to **67**, whereas at higher phosphor content, greater initiator concentrations seem to be required to achieve cross-linking, which in turn requires higher temperature treatment (> 200 °C) to remove the amine radical cations formed from photo-induced electron transfer from **64** to the initiator, which leads to some decomposition of the emitter. Accordingly,

the 15% used represents a compromise between these considerations. Finally, a PBD/poly(methyl methacrylate) blend was used as a solution-processed ETL. A maximum

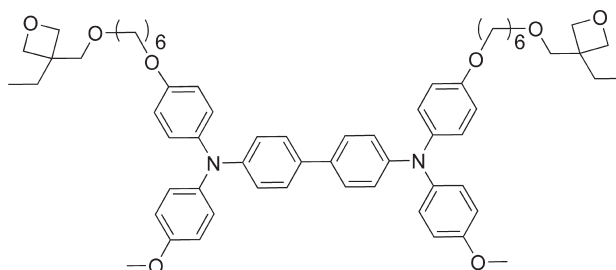


64

Figure 29. Small molecule oxetane-functionalized bis(diarylamino)-biphenyl used in a comparison with the polymers shown in Figure 28.

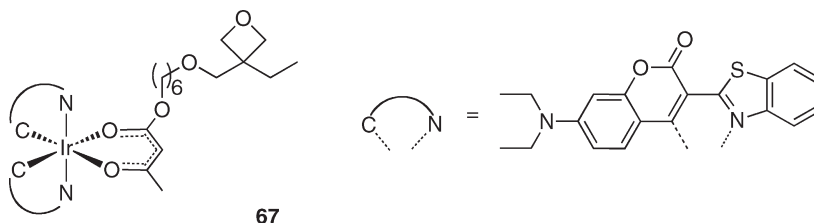


65



66

Figure 30. Additional examples of oxetane-functionalized bis(diarylamino)biphenyl derivatives.



67

Figure 31. Oxetane-functionalized Ir-based orange emitter.

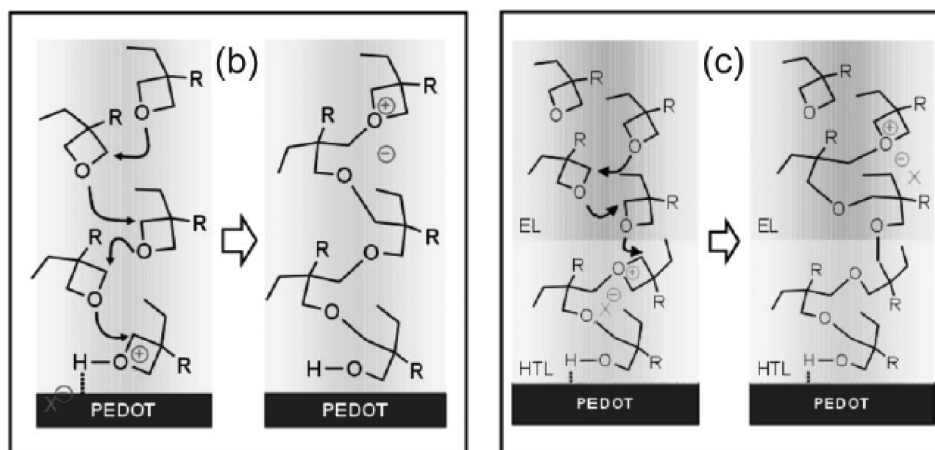
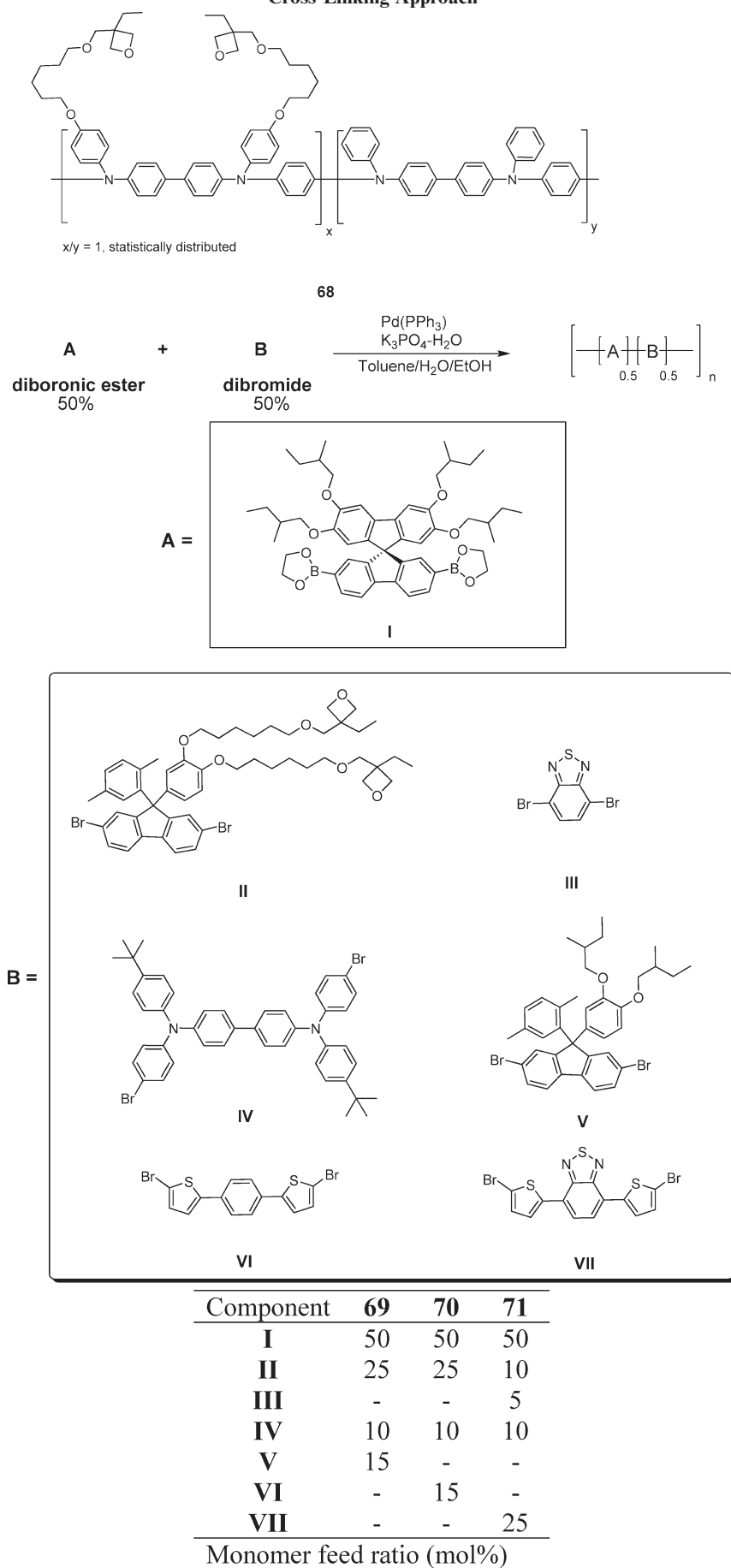


Figure 32. Schematic of the layer-by-layer cross-linking approach. Reproduced with permission from ref 68. Copyright Wiley-VCH Verlag GmbH & Co. KGaA.

luminance efficiency of 18.4 cd/A was obtained at a voltage of 5 V and a brightness of 100 cd/m², with a maximum power efficiency of 15 lm/W; these efficiencies are excellent for solution-processed devices, approaching those seen for the best vacuum-deposited orange devices. Additional devices with no hole-transport layer, or with a single hole-transport layer, performed somewhat more poorly, whereas the presence of the ETL is particularly important, with a device omitting this exhibiting ca. 30 times poorer luminance efficiency.

In 2009,⁶⁸ Köhnen et al. reported a variation on the oxetane approach, which they referred to as “layer-by-layer cross-linking”. This is shown schematically in Figure 32; oxonium ions present at the surface of a layer following cross-linking can potentially initiate cross-linking in a subsequent oxetane layer solution processed on top. Moreover, in this study, rather than initiating the cross-linking of the first layer using a photoacid, the

Scheme 14. Polymer Scheme, Components, and Feed Ratios Used in the Synthesis of Materials for Use in the Layer-by-Layer Cross-Linking Approach

process was initiated by sulfonic acid groups present in the PEDOT-PSS layer. The hole-transporting and emissive polymers evaluated are shown in Scheme 14. The process of cross-linking the films was achieved by spin-casting oxetane-functionalized copolymers onto PEDOT-PSS, followed by a heating step (100–200 °C), which is believed to cause the CROP-based cross-linking reaction of the oxetanes to proceed upward through the layer. Coulombic attraction between the charged reactive cationic oxonium species and the anionic PEDOT component does not appear to limit the CROP process as high thicknesses (> 100 nm) could be achieved. The authors suggested that a counteranion, such as a sulfate ion resulting from decomposition in the PEDOT-PSS layer, migrates through the layer accompanying cationic reactive oxonium species. Indeed, addition of a salt or excess poly(styrene sulfonic acid) to the cross-linking layer led to an increased rate of cross-linking as well as thicker films. The authors noted that the most effective cross-linking temperature should be near or above the glass transition of the material used. Following cross-linking of the initial layer, it was found that subsequent layers could also be cross-linked, thus permitting the solution-processing of multilayer devices from solution in which each layer is cross-linked, not only within the layer, but also to the adjacent organic layers, thus, presumably leading to highly robust organic–organic interfaces.

A white OLED was fabricated with the multilayer architecture: ITO/PEDOT-PSS(35 nm)/**68**(20 nm)/**71**(5 nm)/**70**(10 nm)/**69**(60 nm)/Ba/Ag. The reported efficiency was 4.5 cd/A at 100 cd/m² and 2.1 cd/A at 1000 cd/m². The device was found to be “near-white” in emission but showed voltage-dependent color. The initial device performance of an OLEDs fabricated using PEDOT-PSS initiation was found to be similar to that for an analogous device fabricated using photo-initiation, but the lifetime was improved in the former device (by a factor of 3.1 for a single layer red OLED (**71**) to an extrapolated half-brightness lifetime of 6200 h). Two blue devices were also evaluated. The first device used a PEDOT-PSS cross-linked **68** and a photochemically cross-linked blue **69** layer. A second device employing the combined PEDOT-PSS-initiated layer-by-layer approach was also fabricated. Compared to a fully photochemically cross-linked control bilayer device, the first device (where the hole-transport layer, **68**, was cross-linked by PEDOT but the emissive layer was photochemically cross-linked) showed a 10% improvement in lifetime, whereas the second device (where layer-by-layer cross-linking was employed) had a lifetime improvement by a factor of 2.1 (to greater than 1000 h). The presence of side products from the photoacid were suggested as a potential reason for decreased lifetime in the reference devices. The PEDOT-PSS/layer-by-layer approach should be free of these species, although the possibility of mobile counteranions within the active layers could lead to its own problems.

Table 5. Comparison of Main Cross-Linking Approaches Used to Date in OLEDs

cross-linker	reaction type	typical conditions	applications to date	potential advantages	potential disadvantages
siloxanes	condensation	moisture	small molecules	room temp. process often spontaneous in air	moisture and side products may affect device lifetime can require curing/annealing step to remove side products
styrenes	polymerization	thermal	small molecules and polymers	enhanced lifetime observed in some examples polymerization reaction: only two groups per molecule required	high temperatures can be necessary can require hours
acrylates	polymerization	UV (via photoinitiator)	small molecules	demonstrated for wide range of active materials polymerization reaction: only two groups per molecule required	possible side products from radical initiator
trifluorovinyl ethers	dimerization	thermal	small molecules and polymers	room temperature process photolithography possible	high temperatures (> 200 °C) necessary can require hours
benzocyclo-butenes	dimerization	thermal	polymers	no reagents or side-products improved device performance seen in some cases	high temperatures (180–250 °C) requires hours
cinnamates/chalcones	dimerization	UV (direct)	polymers	improved device characteristics observed rapid room-temperature process	potentially challenging to achieve cross-linking without causing photodamage to transport material
oxetane	polymerization	acid (UV-photoacid or PEDOT-PSS)	small molecules or polymers	no reagents or side-products photolithography possible rapid reaction, sometimes at low temperatures low shrinkage photolithography possible	possibility of side products and/or mobile ions heating can be required

Conclusions

This review of the literature concerning cross-linkable organic materials for OLED applications has shown that they can play a useful role in simplifying the fabrication of multilayer devices by solution-processing. A wide range of different cross-linking chemistries have been investigated to insolubilize both small molecules and polymers and, in some cases, highly efficient devices with EQEs approaching 20% have been achieved using these cross-linked materials. A range of factors should be considered in selecting a cross-linking approach, some of these are summarized in Table 5 and discussed in the following paragraphs.

Although siloxanes show rapid cross-linking under relatively mild conditions, this approach has not been adopted widely in recent work, perhaps due to understandable concerns regarding possible adverse affects associated with the presence of water and/or condensation side products. The recently reported PEDOT-PSS-initiated polymerization of oxetanes also proceeds under relatively mild conditions and presumably low temperatures could be used in the case of low- T_g materials. However, most studies have used cross-linking chemistry that is thermally or photochemically activated.

Of the groups that have been used as thermal cross-linkers, styryl groups require temperatures above 150 °C and heating times ranging from minutes to hours. These groups seem promising based on the literature reports showing their application to a great diversity of groups having a variety of device functions. Trifluorovinyl ether and benzocyclobutene thermal cross-linkers provide an alternative to the styryl group but generally require higher temperatures (> 200 °C) and, for some examples, heating times of several hours. The need for such long heating steps can be an issue and the high temperatures needed could have detrimental effects on the electroactive components of the OLED devices. Moreover, the polymeric, rather than dimeric, nature of cross-linking obtainable with styrenes means that fewer reactive groups per small molecule (2 vs 3 or more for TFVE and BCB groups) are required for cross-linking. On the other hand, fewer side products or defects might be anticipated to be formed by the dimerization of TFVE and BCB groups than by the polymerization of styrenes.

Three very different UV-initiated cross-linking chemistries have been utilized in OLEDs: the radical polymerization of acrylates and the cationic polymerization of oxetanes have been initiated by photoradical-generators and photo-acid-generators, respectively, whereas the dimerization of chalcones and cinnamates occurs by direct photoexcitation of the cross-linking groups. UV cross-linking offers the potential for pixelation and other patterning using standard lithographic procedures. However, achieving sufficient cross-linking without photodamage to the active materials (which may result in side products with adverse effects on device performance or lifetime) can be challenging in some cases, especially where absorptions of the photoinitiator or photo-cross-linkable group overlap with those of the

active material and the latter do not sensitize the former. Although the use of photochemistry offers the potential to avoid the high temperatures associated with thermal cross-linking, in the case of oxetane polymerization a heating step is also often found to be useful in driving the photochemically initiated reaction toward completion. The oxetane and cinnamate/chalcone approaches are attractive in that these groups are inert under radical polymerization conditions and so can be readily incorporated as side chains into main-chain acrylate or styrene polymers. Photopolymerization of both acrylates and oxetanes produce additional products from the photoinitiators, which could potentially interfere with device performance.

Despite the range of cross-linking chemistries discussed above, we are unaware of any study that directly compares alternative cross-linking methods using comparable materials and devices. Such studies would be of great value to the OLED community, especially if conducted using a range of active materials with different device functions and susceptibility to side reactions. Moreover, there is, in general, a paucity of device lifetime data for cross-linked OLEDs, with only a limited number of studies reporting comparable lifetimes to analogous non-cross-linked devices and even fewer in which these lifetimes are promising for potential applications. The availability of more data of this type in the public domain would be very helpful in assessing the potential utility of cross-linking.

Acknowledgment. The authors thank Solvay S.A. for supporting some of our work in this area.

Abbreviations Used

AFM, atomic force microscopy
 Alq₃, tris(8-hydroxyquinolino)aluminum
 BCB, benzocyclobutene
 DSC, differential scanning calorimetry
 EQE, external quantum efficiency
 EL, electroluminescence
 EML, emissive layer
 ETL, electron-transport layer
 IP, ionization potential
 IR, infrared
 ITO, indium tin oxide
 OLED, organic light-emitting diode
 PBD, 2-(4-biphenyl)-5-(4-*tert*-butylphenyl)-3,4-oxadiazole
 PEDOT-PSS, poly(3,4-ethylenedioxythiophene) poly(styrenesulfonate)
 PL, photoluminescence
 PPV, poly(*p*-phenylenevinylene)
 PVK, poly(*N*-vinylcarbazole)
 TFVE, trifluorovinyl ether
 TGA, thermogravimetric analysis
 TPBI, 1,3,5-tris(*N*-phenylbenzimidazol-2-yl)benzene
 TPD, 4,4'-bis(*m*-tolylphenylamino)biphenyl
 UV-vis, ultraviolet-visible

References

- (1) Ma, B.; Lauterwasser, F.; Deng, L.; Zonte, C. S.; Kim, B. J.; Fréchet, J. M. J. *Chem. Mater.* **2007**, *19*, 4827.
- (2) So, F.; Kido, J.; Burrows, P. *MRS Bull.* **2008**, *33*, 663.
- (3) Tang, C. W.; Van Slyke, S. A. *Appl. Phys. Lett.* **1987**, *51*, 913.
- (4) Hung, L. S.; Chen, C. H. *Mater. Sci. Eng., R* **2002**, *39*, 143.
- (5) Baldo, M. A.; Lamansky, S.; Burrows, P. E.; Forrest, S. R. *Appl. Phys. Lett.* **1999**, *75*, 4.
- (6) Li, Y.-J.; Sasabe, H.; Su, S.-J.; Tanaka, D.; Takeda, T.; Pu, Y.-J.; Kido, J. *Chem. Lett.* **2010**, *39*, 140.
- (7) Kanno, H.; Giebink, N. C.; Forrest, S. R. *Appl. Phys. Lett.* **2006**, *89*, 023503.
- (8) Lin, W.-C.; Wang, W.-B.; Lin, Y.-C.; Yu, B.-Y.; Chen, Y.-Y.; Hsu, M.-F.; Jou, J.-H.; Shyue, J.-J. *Org. Electron.* **2009**, *10*, 581.
- (9) Carter, S. A.; Angelopoulos, M.; Karg, S.; Brock, P. J.; Scott, J. C. *Appl. Phys. Lett.* **1997**, *70*, 2067.
- (10) Kim, W. H.; Mäkinen, A. J.; Nikolov, N.; Shashidhar, R.; Kim, H.; Kafafi, Z. H. *Appl. Phys. Lett.* **2002**, *80*, 3844.
- (11) Hwang, M.-Y.; Hua, M.-Y.; Chen, S.-A. *Polymer* **1999**, *40*, 3233.
- (12) Ma, W.; Iyer, P. K.; Gong, X.; Liu, B.; Moses, D.; Bazan, G. C.; Heeger, A. J. *Adv. Mater.* **2005**, *17*, 274.
- (13) Zhang, Y.; Huang, F.; Chi, Y.; Jen, A. K.-Y. *Adv. Mater.* **2008**, *20*, 1565.
- (14) Garcia, A.; Yang, R.; Jin, Y.; Walker, B.; Nguyen, T.-Q. *Appl. Phys. Lett.* **2007**, *91*, 153502.
- (15) Zhang, Y.; Huang, F.; Jen, A. K.-Y.; Chi, Y. *Appl. Phys. Lett.* **2008**, *92*, 063303.
- (16) Burroughes, J. H.; Bradley, D. D. C.; Brown, A. R.; Marks, R. N.; Mackay, K.; Friend, R. H.; Burn, P. L.; Holmes, A. B. *Nature* **1990**, *347*, 539.
- (17) Nuyken, O.; Bacher, E.; Braig, T.; Fáber, R. M.; F.; Rojahn, M.; Wiederhorn, V.; Meerholz, K.; Müller, D. *Des. Monomers Polym.* **2002**, *5*, 195.
- (18) Nuyken, O.; Jungermann, S.; Wiederhorn, V.; Bacher, E.; Meerholz, K. *Monatsh. Chem.* **2006**, *137*, 811.
- (19) Huang, F.; Cheng, Y.-J.; Zhang, Y.; Liu, M. S.; Jen, A. K.-Y. *J. Mater. Chem.* **2008**, *18*, 4495.
- (20) Shieh, Y.-T.; Hsiao, K.-I. *J. Appl. Polym. Sci.* **1998**, *70*, 1075.
- (21) Li, W.; Wang, Q.; Cui, J.; Chou, H.; Shaheen, S. E.; Jabbour, G. E.; Anderson, J.; Lee, P.; Kippelen, B.; Peyghambarian, N.; Armstrong, N. R.; Marks, T. J. *Adv. Mater.* **1999**, *11*, 730.
- (22) Yan, H.; Scott, B. J.; Huang, Q.; Marks, T. J. *Adv. Mater.* **2004**, *16*, 1948.
- (23) Lee, S.; Lyu, Y.-Y.; Lee, S.-H. *Synth. Met.* **2006**, *156*, 1004.
- (24) Weinfurter, K.-H.; Fujikawa, H.; Tokito, S.; Taga, Y. *Appl. Phys. Lett.* **2000**, *76*, 2502.
- (25) Becker, K.; Lupton, J. M.; Feldmann, J.; Nehls, B. S.; Galbrecht, F.; Gao, D.; Scherf, U. *Adv. Funct. Mater.* **2006**, *16*, 364.
- (26) Klarner, G.; Lee, J.-I.; Lee, V. Y.; Chan, E.; Chen, J.-P.; Nelson, A.; Markiewicz, D.; Siemens, R.; Scott, J. C.; Miller, R. D. *Chem. Mater.* **1999**, *11*, 1800.
- (27) Marsitzky, D.; Murray, J.; Scott, J. C.; Carter, K. R. *Chem. Mater.* **2001**, *13*, 4285.
- (28) Bozano, L. D.; Carter, K. R.; Lee, V. Y.; Miller, R. D.; DiPietro, R.; Scott, J. C. *J. Appl. Phys.* **2003**, *94*, 3061.
- (29) Dailey, S.; Feast, W. J.; Peace, R. J.; Sage, I. C.; Till, S.; Wood, E. L. *J. Mater. Chem.* **2001**, *11*, 2238.
- (30) Sun, H.; Liu, Z.; Hu, Y.; Wang, L.; Ma, D.; Jing, X.; Wang, F. *J. Polym. Sci., Part A: Polym. Chem.* **2004**, *42*, 2124.
- (31) Grimsdale, A. C.; Chan, K. L.; Martin, R. E.; Jokisz, P. G.; Holmes, A. B. *Chem. Rev.* **2009**, 897.
- (32) Paul, G. K.; Mwaura, J.; Argun, A. A.; Taranekekar, P.; Reynolds, J. R. *Macromolecules* **2006**, *39*, 7789.
- (33) Niu, Y.-H.; Liu, M. S.; Ka, J.-W.; Bardeker, J.; Zin, M. T.; Schofield, R.; Chi, Y.; Jen, A. K.-Y. *Adv. Mater.* **2007**, *19*, 300.
- (34) Kim, J. S.; Friend, R. H.; Grizzi, I.; Burroughes, J. H. *Appl. Phys. Lett.* **2005**, *87*, 023506.
- (35) Cheng, Y.-J.; Liu, M. S.; Zhang, Y.; Niu, Y.; Huang, F.; Ka, J.-W.; Yip, H.-L.; Tian, Y.; Jen, A. K.-Y. *Chem. Mater.* **2008**, *20*, 413.
- (36) Ma, B.; Kim, B. J.; Poulsen, D. A.; Pastine, S. J.; Fréchet, J. M. J. *Adv. Funct. Mater.* **2009**, *19*, 1024.
- (37) Bacher, A.; Erdelen, C. H.; Paulus, W.; Ringsdorf, H.; Schmidt, H.-W.; Schuhmacher, P. *Macromolecules* **1999**, *32*, 4551.
- (38) Bacher, A.; Bleyl, I.; Erdelen, C. H.; Haarer, D.; Paulus, W.; Schmidt, H.-W. *Adv. Mater.* **1997**, *9*, 1031.
- (39) Du, N.; Tian, R.; Peng, J.; Mei, Q.; Lu, M. *Macromol. Rapid Commun.* **2006**, *27*, 412.
- (40) Ji, J.; Narayan-Sarathy, S.; Neilson, R. H.; Oxley, J. D.; Babb, D. A.; Rondan, N. G.; Smith, D. W., Jr. *Organometallics* **1998**, *17*, 783.
- (41) Smith, D. W.; Babb, D. A. *Macromolecules* **1996**, *29*, 852.
- (42) Niu, Y.-H.; Liu, M. S.; Ka, J.-W.; Jen, A. K.-Y. *Appl. Phys. Lett.* **2006**, *88*, 093505.
- (43) Lim, B.; Hwang, J.-T.; Kim, J. Y.; Ghim, J.; Vak, D.; Noh, Y.-Y.; Lee, S.-H.; Lee, K.; Heeger, A. J.; Kim, D.-Y. *Org. Lett.* **2006**, *8*, 4703.
- (44) Cava, M. P.; Deana, A. A. *J. Am. Chem. Soc.* **1959**, *81*, 4266.
- (45) Nakayama, Y.; Matsuda, T. *J. Polym. Sci., Part A* **1992**, *30*, 2451.
- (46) Rehab, A.; Salahuddin, N. *Polymer* **1999**, *40*, 2197.
- (47) Li, X.-C.; Yong, T.-M.; Gruner, J.; Holmes, A. B.; Moratti, S. C.; Cacialli, F.; Friend, R. H. *Synth. Met.* **1997**, *84*, 437.
- (48) Zhang, Y.-D.; Hreha, R. D.; Jabbour, G. E.; Kippelen, B.; Peyghambarian, N.; Marder, S. R. *J. Mater. Chem.* **2002**, *12*, 1703.
- (49) Bellmann, E.; Shaheen, S. E.; Thayumanavan, S.; Barlow, S.; Grubbs, R. H.; Marder, S. R.; Kippelen, B.; Peyghambarian, N. *Chem. Mater.* **1998**, *10*, 1668.
- (50) Domercq, B.; Hreha, R. D.; Zhang, Y.-D.; Larribeau, N.; Haddock, J. N.; Schultz, C.; Marder, S. R.; Kippelen, B. *Chem. Mater.* **2003**, *15*, 1491.
- (51) Zhan, X.; Haldi, A.; Yu, J.; Kondo, T.; Domercq, B.; Cho, J.-Y.; Barlow, S.; Kippelen, B.; Marder, S. R. *Polymer* **2009**, *50*, 397.
- (52) Cho, J.-Y.; Domercq, B.; Barlow, S.; Suponitsky, K. Y.; Li, J.; Timofeeva, T. V.; Jones, S. C.; Hayden, L. E.; Kimyonok, A.; South, C. R.; Weck, M.; Kippelen, B.; Marder, S. R. *Organometallics* **2007**, *26*, 4816.
- (53) Kimyonok, A.; Domercq, B.; Haldi, A.; Cho, J.-Y.; Carlise, J. R.; Wang, X.-Y.; Hayden, L. E.; Jones, S. C.; Barlow, S.; Marder, S. R.; Kippelen, B.; Weck, M. *Chem. Mater.* **2007**, *19*, 5602.
- (54) Haldi, A.; Kimyonok, A.; Domercq, B.; Hayden, L. E.; Jones, S. C.; Marder, S. R.; Weck, M.; Kippelen, B. *Adv. Funct. Mater.* **2008**, *18*, 3056.
- (55) Crivello, J. V.; Falk, B.; Zonca, M. R. *J. Polym. Sci., Part A* **2004**, *42*, 1630.
- (56) Dektar, J. L.; Hacker, N. P. *J. Am. Chem. Soc.* **1990**, *112*, 6004.
- (57) Pappas, S. P.; Pappas, B. C.; Gatechair, L. R.; Jilek, J. H. *Polym. Photochem.* **1984**, *5*, 1.
- (58) Dektar, J. L.; Hacker, N. P. *J. Photochem. Photobiol. A* **1989**, *46*, 233.
- (59) Crivello, J. V.; Bulut, U. *J. Polym. Sci., Part A* **2005**, *43*, 5217.
- (60) Nuyken, O.; Bohner, R.; C. E. *Macromol. Symp.* **1996**, *107*, 125.
- (61) Bayerl, M. S.; Braig, T.; Nuyken, O.; Müller, D.; Gross, M.; Meerholz, K. *Macromol. Rapid Commun.* **1999**, *20*, 224.
- (62) Sangermano, M.; Giannelli, S.; Acosta Ortiz, R.; Berlanga Duarte, M. L.; Rueda Gonzalez, A. K.; Garcia Valdez, A. E. *J. Appl. Polym. Sci.* **2009**, *112*, 1780.
- (63) Müller, C. D.; Falcou, A.; Reckefuss, N.; Rojahn, M.; Wiederhorn, V.; Rudati, P.; Frohne, H.; Nuyken, O.; Becker, H.; Meerholz, K. *Nature* **2003**, *421*, 829.
- (64) Bacher, E.; Jungermann, S.; Rojahn, M.; Wiederhorn, V.; Nuyken, O. *Macromol. Rapid Commun.* **2004**, *25*, 1191.
- (65) Bacher, E.; Bayerl, M. S.; Rudati, P.; Reckefuss, N.; Müller, C. D.; Meerholz, K.; Nuyken, O. *Macromolecules* **2005**, *38*, 1640.
- (66) Yang, X.; Müller, D.; Neher, D.; Meerholz, K. *Adv. Mater.* **2006**, *18*, 948.
- (67) Rehmann, N.; Ulbricht, C.; Köhnen, A.; Zacharias, P.; Gather, M. C.; Hertel, D.; Holder, E.; Meerholz, K.; Schubert, U. S. *Adv. Mater.* **2008**, *20*, 129.
- (68) Köhnen, A.; Riegel, N.; Kremer, J. H.-W.; Lademann, H.; Müller, D. C.; Meerholz, K. *Adv. Mater.* **2009**, *21*, 879.